2025년 한국고에너지물리학회 및 핵-입자-천체분과 연합 워크샵

11월 19일 – 22일, 2025
전남대학교

Exploring Nuclear Ground-State Energy with IBM Quantum Computers

Jubin Park (Soongsil University)

Collaborators: Prof. Myung-Ki Cheoun, Ms. Chae-hyun yoon, Mr. Minkyu Lee

Outline

- Introduction to Quantum Computing
  - Gate-based (IBM Q, IonQ)
  - Quantum Annealing (D-Wave)
  - NISQ 시대의 한계와 하드웨어 발전(IBM Eagle → Heron → Nighthawk)
- Variational Quantum Eigensolver (VQE)
  - Ansatz, Pauli decomposition
  - UCC, QCC, BK/JW mapping
  - IBM Q 기반 실험 환경
- Results (IBM Q) : Deuteron Ground-State Calculation
  - Deuteron binding energy vs ancillary qubits (Quantum Annealing)
  - 2-qubit Hamiltonian (PRL 2018)
    (– 1-qubit reduced Hamiltonian)
  - 최신 IBM backend (Heron)에서의 시뮬레이션 & noise 문제
- Conclusions & Outlook

- Introduction to Quantum Computer

D-wave Quantum Annealer

→ D-wave Advantage 2 (2023)

→ 7000++ qubit

→ High applicability and accuracy of quantum measurement

→ **Programming difficulty**

→ Require more qubits

IBM-Q, ION-Q

→ IBM-Q, Ion-Q

→ 400++ qubit

→ Large quantum error

→ **Programmable**

→ Require more qubits

Noisy Intermediate-Scale Quantum (NISQ)

※ 당분간의 양자컴퓨터 시대를 NISQ area라고 부르는데, 이 뜻은 적당한 큐빗 수(~1000개)이면서, 에러를 제거할 수 없는 양자컴퓨터를 말한다.

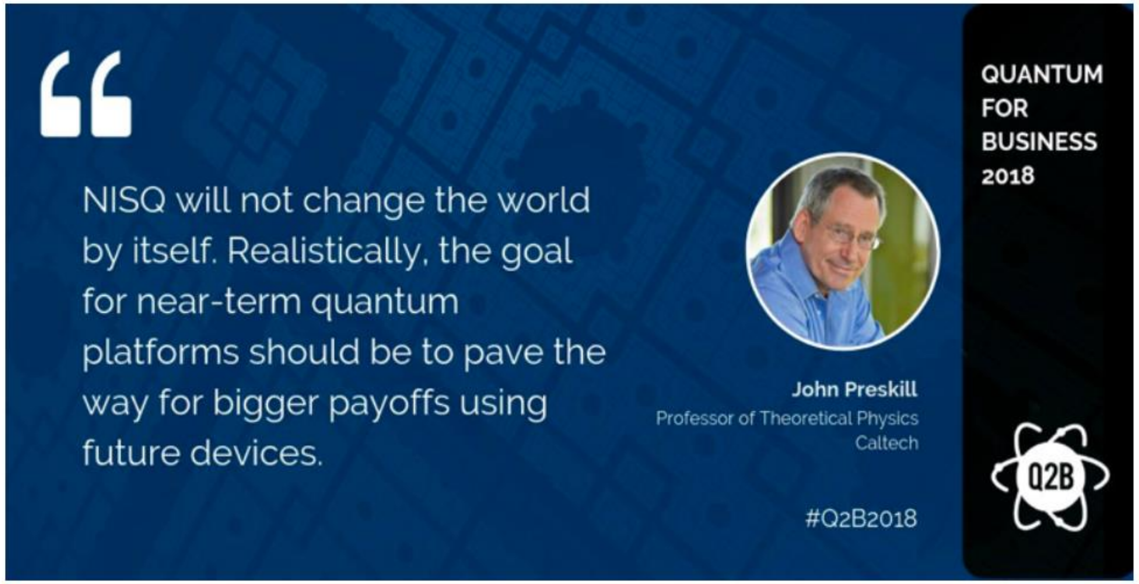

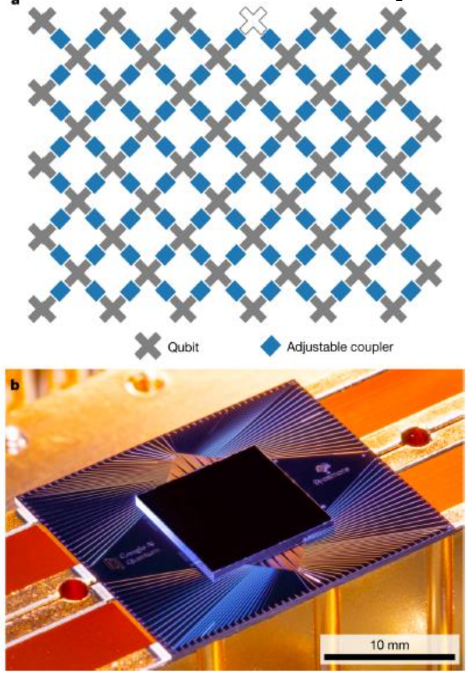

Google's Sycamore Processor

- 최근 양자정보 연구동향/비전: 국소적, 작업-편중형(Task-Oriented)
- 양자연산의 기능적 최적화 → 측정데이터/확률분포에의 양자효과 분석/활용 (e.g., 샘플링 문제)
- *NISQ 시대 도래:
  - 오류를 허용하고(Noisy)
  - 중규모에서(Intermediate-Scale)에서
  - 실현 가능한 형태의 양자(Quantum) 기술의 추구

방정호 박사님(한국전자통신연구원) 발표자료

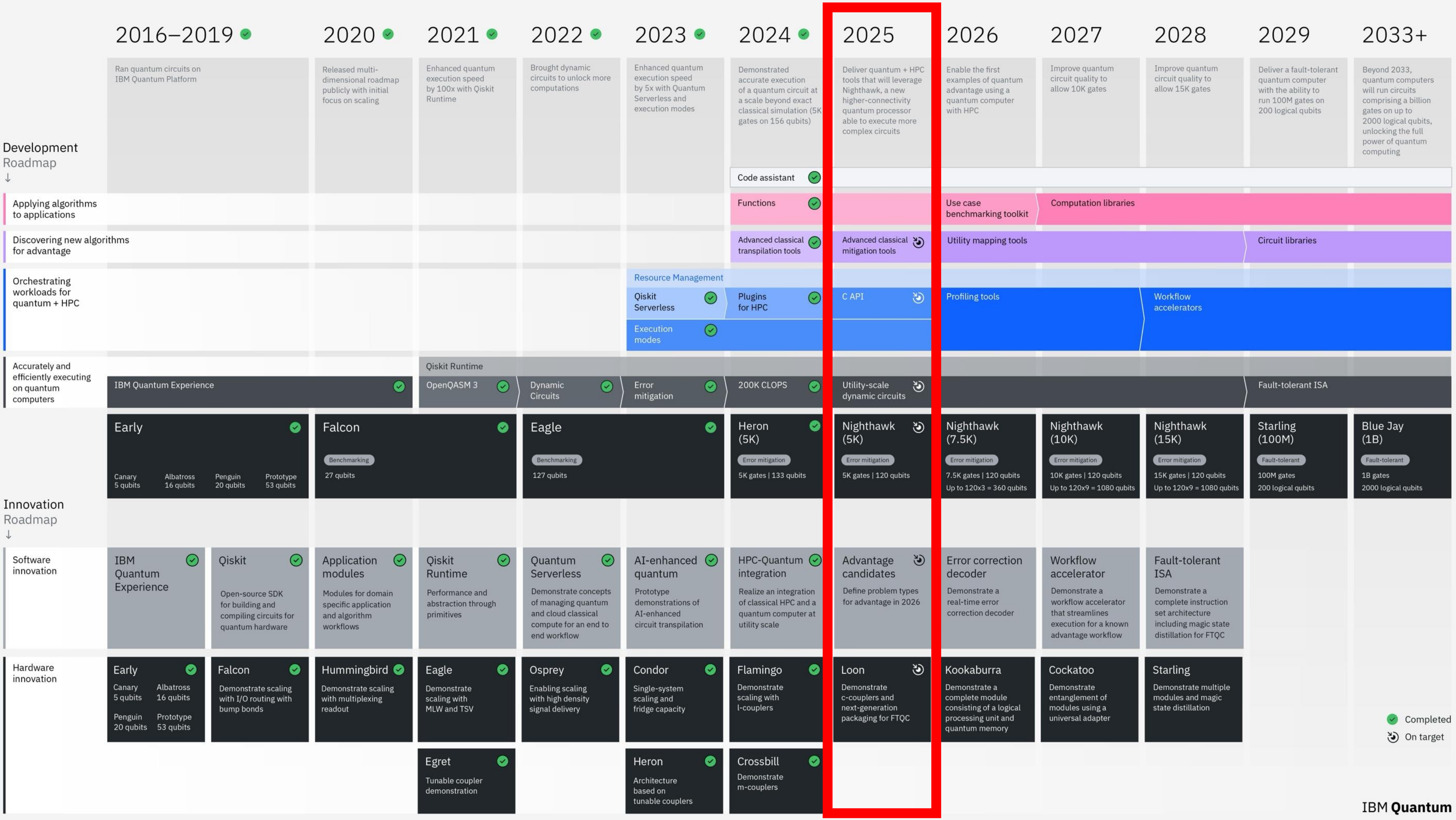
2016–2019
2020
2021
2022
2023
2024
2025
2026
2027
2028
2029
2033+
Ran quantum circuits on IBM Quantum Platform
Released multi-dimensional roadmap publicly with initial focus on scaling
Enhanced quantum execution speed by 100x with Qiskit Runtime
Brought dynamic circuits to unlock more computations
Enhanced quantum execution speed by 5x with Quantum Serverless and execution modes
Demonstrated accurate execution of a quantum circuit at a scale beyond exact classical simulation (5K gates on 156 qubits)
Deliver quantum + HPC tools that will leverage Nighthawk, a new higher-connectivity quantum processor able to execute more complex circuits
Enable the first examples of quantum advantage using a quantum computer with HPC
Improve quantum circuit quality to allow 10K gates
Improve quantum circuit quality to allow 15K gates
Deliver a fault-tolerant quantum computer with the ability to run 100M gates on 200 logical qubits
Beyond 2033, quantum computers will run circuits comprising a billion gates on up to 2000 logical qubits, unlocking the full power of quantum computing
Development Roadmap
Code assistant
Applying algorithms to applications
Functions
Use case benchmarking toolkit
Computation libraries
Discovering new algorithms for advantage
Advanced classical transpilation tools
Advanced classical mitigation tools
Utility mapping tools
Circuit libraries
Orchestrating workloads for quantum + HPC
Resource Management
Qiskit Serverless
Plugins for HPC
C API
Profiling tools
Workflow accelerators
Execution modes
Accurately and efficiently executing on quantum computers
Qiskit Runtime
IBM Quantum Experience
OpenQASM 3
Dynamic Circuits
Error mitigation
200K CLOPS
Utility-scale dynamic circuits
Fault-tolerant ISA
Early
Canary 5 qubits
Albatross 16 qubits
Penguin 20 qubits
Prototype 53 qubits
Falcon
Benchmarking
27 qubits
Eagle
Benchmarking
127 qubits
Heron (5K)
Error mitigation
5K gates | 133 qubits
Nighthawk (5K)
Error mitigation
5K gates | 120 qubits
Nighthawk (7.5K)
Error mitigation
7.5K gates | 120 qubits
Up to 120x3 = 360 qubits
Nighthawk (10K)
Error mitigation
10K gates | 120 qubits
Up to 120x9 = 1080 qubits
Nighthawk (15K)
Error mitigation
15K gates | 120 qubits
Up to 120x9 = 1080 qubits
Starling (100M)
Fault-tolerant
100M gates
200 logical qubits
Blue Jay (1B)
Fault-tolerant
1B gates
2000 logical qubits
Innovation Roadmap
Software innovation
IBM Quantum Experience
Qiskit
Open-source SDK for building and compiling circuits for quantum hardware
Application modules
Modules for domain specific application and algorithm workflows
Qiskit Runtime
Performance and abstraction through primitives
Quantum Serverless
Demonstrate concepts of managing quantum and cloud classical compute for an end to end workflow
AI-enhanced quantum
Prototype demonstrations of AI-enhanced circuit transpilation
HPC-Quantum integration
Realize an integration of classical HPC and a quantum computer at utility scale
Advantage candidates
Define problem types for advantage in 2026
Error correction decoder
Demonstrate a real-time error correction decoder
Workflow accelerator
Demonstrate a workflow accelerator that streamlines execution for a known advantage workflow
Fault-tolerant ISA
Demonstrate a complete instruction set architecture including magic state distillation for FTQC
Hardware innovation
Early
Canary 5 qubits
Albatross 16 qubits
Penguin 20 qubits
Prototype 53 qubits
Falcon
Demonstrate scaling with I/O routing with bump bonds
Hummingbird
Demonstrate scaling with multiplexing readout
Eagle
Demonstrate scaling with MLW and TSV
Osprey
Enabling scaling with high density signal delivery
Condor
Single-system scaling and fridge capacity
Flamingo
Demonstrate scaling with l-couplers
Loon
Demonstrate c-couplers and next-generation packaging for FTQC
Kookaburra
Demonstrate a complete module consisting of a logical processing unit and quantum memory
Cockatoo
Demonstrate entanglement of modules using a universal adapter
Starling
Demonstrate multiple modules and magic state distillation
Egret
Tunable coupler demonstration
Heron
Architecture based on tunable couplers
Crossbill
Demonstrate m-couplers
Completed
On target
IBM Quantum

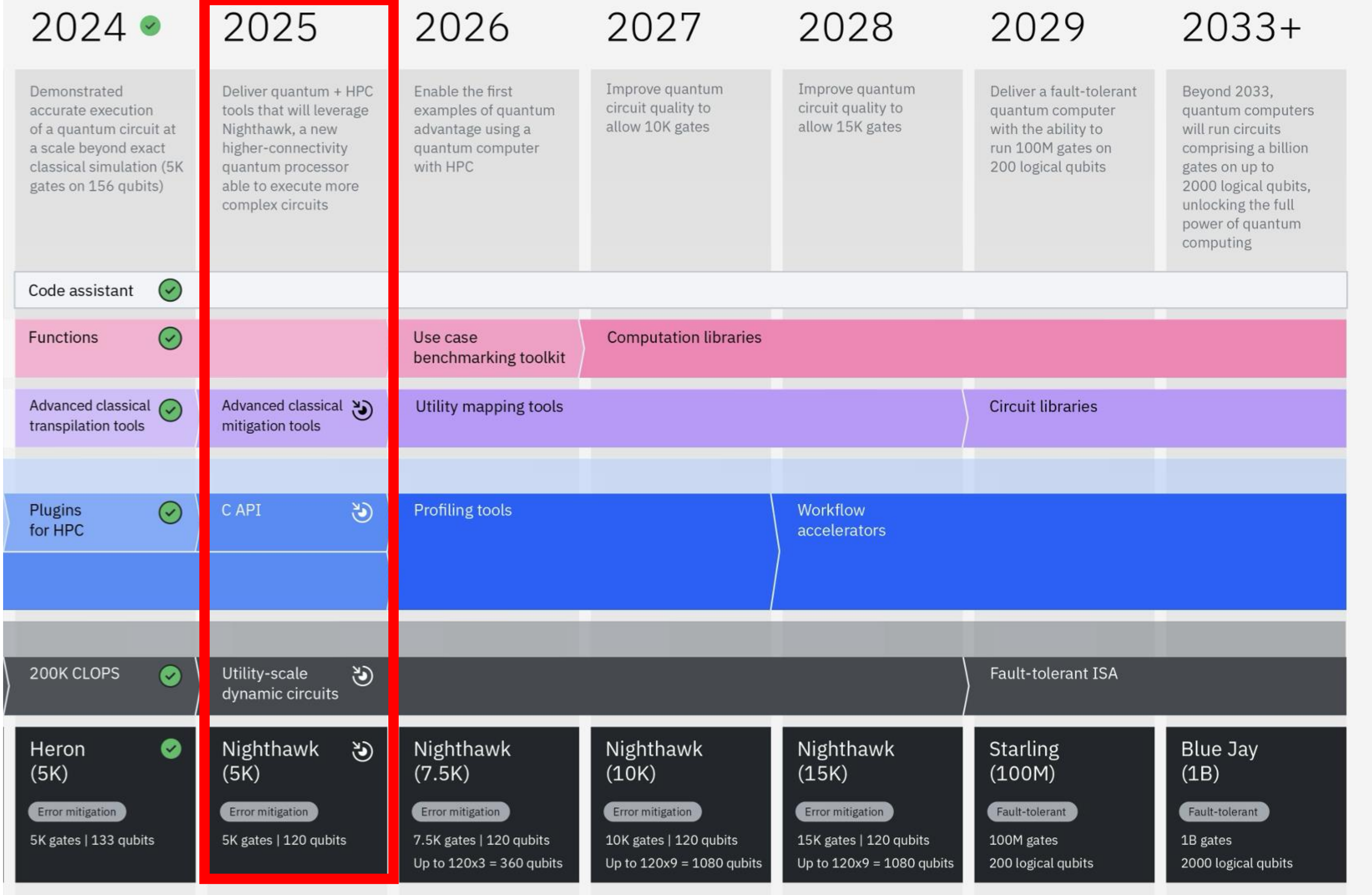
2024
2025
2026
2027
2028
2029
2033+
Demonstrated accurate execution of a quantum circuit at a scale beyond exact classical simulation (5K gates on 156 qubits)
Deliver quantum + HPC tools that will leverage Nighthawk, a new higher-connectivity quantum processor able to execute more complex circuits
Enable the first examples of quantum advantage using a quantum computer with HPC
Improve quantum circuit quality to allow 10K gates
Improve quantum circuit quality to allow 15K gates
Deliver a fault-tolerant quantum computer with the ability to run 100M gates on 200 logical qubits
Beyond 2033, quantum computers will run circuits comprising a billion gates on up to 2000 logical qubits, unlocking the full power of quantum computing
Code assistant
Functions
Use case benchmarking toolkit
Computation libraries
Advanced classical transpilation tools
Advanced classical mitigation tools
Utility mapping tools
Circuit libraries
Plugins for HPC
C API
Profiling tools
Workflow accelerators
200K CLOPS
Utility-scale dynamic circuits
Fault-tolerant ISA
Heron (5K)
Error mitigation
5K gates | 133 qubits
Nighthawk (5K)
Error mitigation
5K gates | 120 qubits
Nighthawk (7.5K)
Error mitigation
7.5K gates | 120 qubits
Up to 120x3 = 360 qubits
Nighthawk (10K)
Error mitigation
10K gates | 120 qubits
Up to 120x9 = 1080 qubits
Nighthawk (15K)
Error mitigation
15K gates | 120 qubits
Up to 120x9 = 1080 qubits
Starling (100M)
Fault-tolerant
100M gates
200 logical qubits
Blue Jay (1B)
Fault-tolerant
1B gates
2000 logical qubits

IBM Quantum

Eagle

IBM Quantum

Heron

Tunable-couplers

With 133 or 156 fixed-frequency qubits and tunable couplers, the Heron family of processors is our highest-performing yet and the core of our System Two architecture.

133/156
Qubits

3.7 E-3
EPLG

250K
CLOPS

View available Heron QPUs ↗

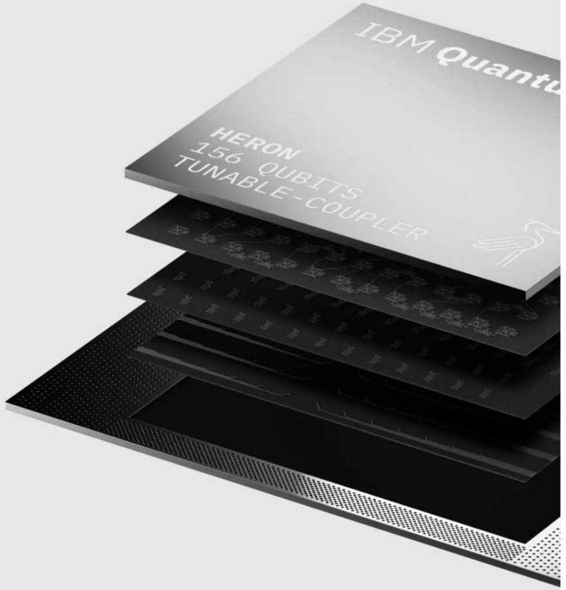

IBM Quantum

Nighthawk

Eagle 의 주요 스펙

✓ 특징

- **127 qubits**
- **Fixed-frequency transmon qubits (고정 주파수 큐비트)**
- **커플러 없음**, 즉 직접 capacitive coupling 구조
- Heron보다 이전 세대의 아키텍처

✓ 핵심 요약

- Eagle은 IBM의 첫 100+ 큐비트 칩
- 그러나 qubit–qubit coupling strength를 조절하는 장치(커플러)가 없어, 2큐빗 게이트 cross-talk, 불필요한 ZZ 상호작용("spectator-ZZ")을 억제하기 어렵다는 단점이 있음.

Heron의 주요 스펙

< Tunable Couplers(조절 가능한 커플러) 탑재 >

- **133 또는 156 qubits**
- **Fixed-frequency qubits + tunable couplers**
- **EPLG = 3.7 × 10^{-3}**
  - 2-qubit error per logical gate에 대응하는 척도
  - 기존 1세대 대비 **오류가 10배 이상 감소**
- **CLOPS = 250K**
  - 큐비트 처리량(양자 프로그램 실행 처리량)

Tunable Coupler가 왜 중요한가?

Heron 세대의 핵심 혁신.

- 두 큐비트 사이의 결합(g_ij)을 **조절**할 수 있음
- 필요할 때만 coupling on, 필요 없으면 off
- 그 결과:
    - **Cross-talk 감소**
    - **불필요한 ZZ 상호작용 억제**
    - **게이트 충돌 현상 감소**
    - **2-qubit gate fidelity 향상**
    - 대규모 양자 회로 실행 시 **스케줄링이 훨씬 쉬워짐**

두 큐비트 사이의 게이트(CNOT, CZ 등)가
얼마나 "정확하게" 의도한 양자연산을 수행하는지를 나타내는 수치.

Heron은 IBM에서 지금까지 가장 안정적이고 노이즈가 적은 프로세서로 평가받음.

https://www.ibm.com/quantum/blog/qdc-2025

IBM Quantum Nighthawk chip (Credit: IBM)

IBM Quantum Nighthawk's qubit plane includes 120 qubits arranged in a square lattice.

Nighthawk (2024–2025 라인업)

✔ 특징

- "Square lattice"라는 구조적 키워드만 제시
- Heron과 같은 tunable-coupler 기반 아키텍처
- 단, **대규모 시스템에서 타일(tile) 형태로 잘 확장되도록 설계한 lattice**
- IBM의 모듈형 시스템(System Two)에서 중요한 역할

✔ 목적

- "대규모 큐비트 칩을 여러 장 연결하여 초대형 양자 시스템 구축"
- 즉 Heron이 단일 칩 성능을 최대화한 칩이라면,

Nighthawk는 '확장성(scalability)'에 최적화된 세대

The information of a logical qubit is encoded across many physical qubits to make it more resilient against errors.

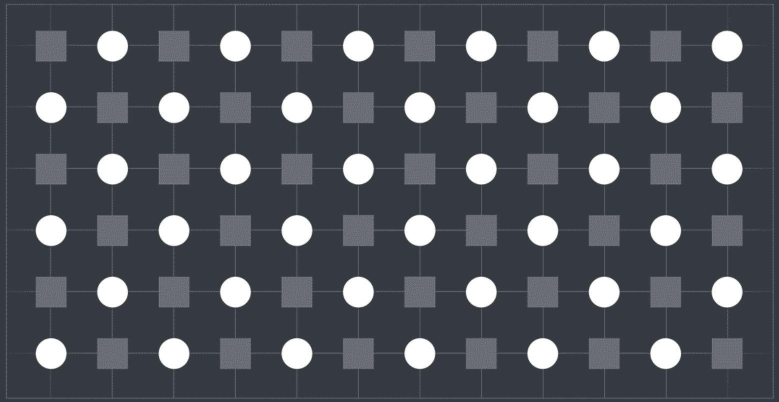

The gross code developed by IBM encodes 12 logical qubits into 144 data qubits, or a 'gross' of data qubits, along with an additional 144 syndrome check qubits. Achieving this on the 2D surface of a quantum chip requires long-range connections between distant qubits within the chip — connections which follow the symmetry of a 3D torus.

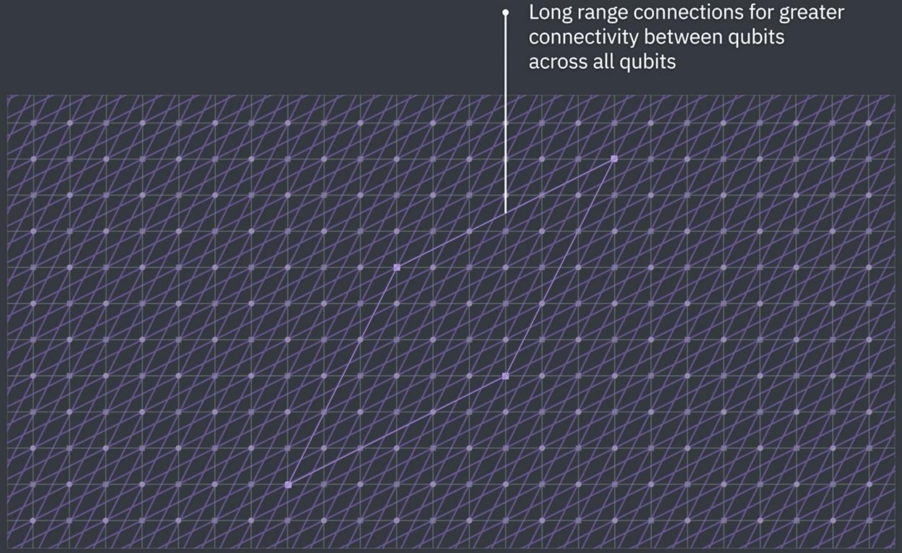

논리 큐비트: 오류보정된(에러 정정되는) 가상 큐비트

※논리 큐비트 1개를 만들기 위해
약 **1,000~10,000개의 물리 큐비트가 필요**
(현재의 물리 게이트 오류율 기준)
※ IBM, Google, Quantinuum, AWS가 모두 이 구조를 사용.

왜 많은 수(예로, 1000개)의 물리 큐비트를 이용해서 1개의 논리 큐비트를 만드는가?

즉, 더 정확하게 정리하면

※ 오류율이 10^{-3}(= 0.1%)

2-qubit gate를 1000번 쓰면:

$$\left(1 - 10^{-3}\right)^{1000} \approx 0.37$$

즉, 10^-3 오류율이면 대략 1000 물리 큐비트 = 1 논리 큐비트

CNOT gate flips the target bit only if the control bit is 1.

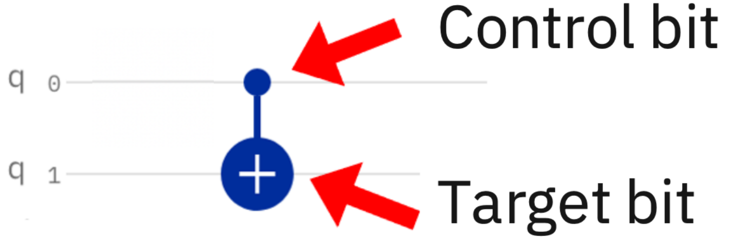

input		output	
Target bit	Control bit	Target bit	Control bit
0	0	0	0
1	0	1	0
0	1	**1**	**1**
1	1	**0**	**1**

양자보정방법의 비유

예: 사람 1000명이 팀(1000개의 물리큐비트)을 이뤄서 한 개의 중요한 정보(1개의 논리큐비트)를 지키는 구조

- 어떤 사람은 말을 잘못 들음 (T1/T2 오류)
- 어떤 사람은 실수로 엉뚱한 말 함 (bit-flip, phase-flip)
- 어떤 사람은 조는 중이라 정보가 날아감 (decoherence)

하지만

1000명이 서로 체크하고 보정하면

원래 정보(= 논리 큐비트)를 유지 가능.

1) T1 (Relaxation Time, 에너지 이완 시간)

정의 : 큐비트가$|1\rangle \rightarrow |0\rangle$로 **자연스럽게 '떨어지는' 데 걸리는 평균 시간**. 즉, 큐비트가 들고 있던 **에너지 자체가 사라져버리는 과정**.

2) T2 (Dephasing Time, 위상 소실 시간)

정의: 큐비트 상태의 **위상(phase) 정보가 흐트러지는 데 걸리는 평균 시간**.$|\psi\rangle = \alpha|0\rangle + e^{i\phi}\beta|1\rangle$

여기서 **위상 φ**가 계속 흔들리면 정보가 손실됨.

C-couplers enable long-range connections between distant qubits within a quantum chip.

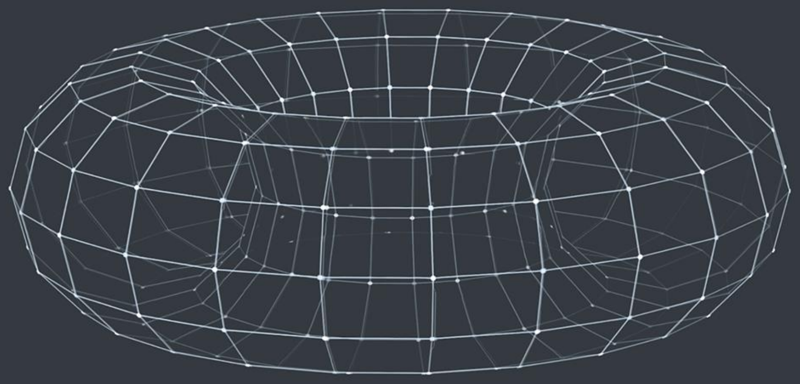

From 2025 to 2028, successive releases of Nighthawk will enable the exploration of increasingly complex quantum circuits.

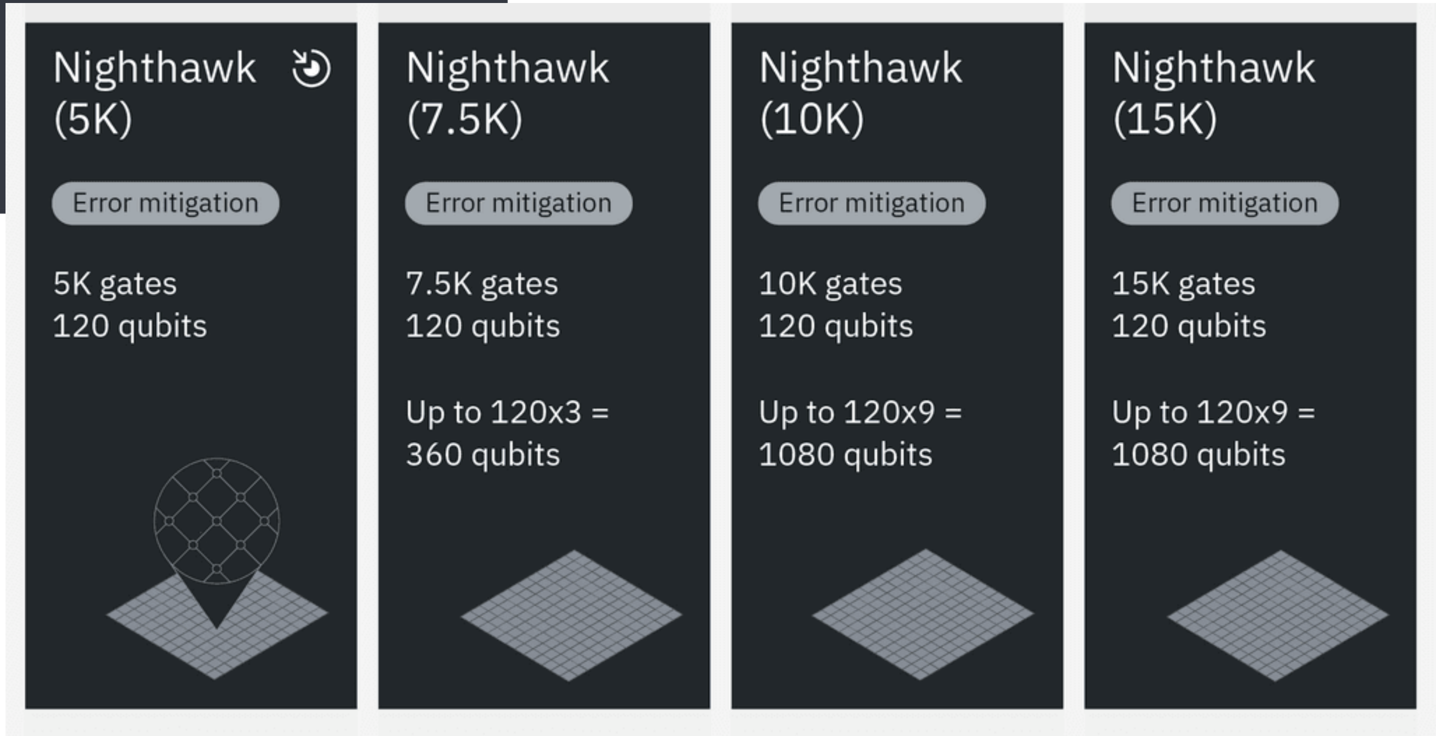

Qubits and quantum gates

$|0\rangle \Rightarrow \boxed{X} \Rightarrow |1\rangle$

NOT Gate

$$X = \begin{bmatrix} 0 & 1 \\ 1 & 0 \end{bmatrix},$$

$$X\,|0\rangle = \begin{bmatrix} 0 & 1 \\ 1 & 0 \end{bmatrix} \begin{bmatrix} 1 \\ 0 \end{bmatrix} = \begin{bmatrix} 0 \\ 1 \end{bmatrix} = |1\rangle$$

Hadamard Gate

$|0\rangle \Rightarrow \boxed{H} \Rightarrow \sqrt{\tfrac{1}{2}} \times |0\rangle + \sqrt{\tfrac{1}{2}} \times |1\rangle$

Creates a superposition

$$H = \frac{1}{\sqrt{2}} \begin{bmatrix} 1 & 1 \\ 1 & -1 \end{bmatrix},$$

$$H\,|0\rangle = \frac{1}{\sqrt{2}} \begin{bmatrix} 1 & 1 \\ 1 & -1 \end{bmatrix} \begin{bmatrix} 1 \\ 0 \end{bmatrix} = \frac{1}{\sqrt{2}} \begin{bmatrix} 1 \\ 1 \end{bmatrix} = \frac{1}{\sqrt{2}} \left(\begin{bmatrix} 1 \\ 0 \end{bmatrix} + \begin{bmatrix} 0 \\ 1 \end{bmatrix} \right) = \frac{1}{\sqrt{2}} (|0\rangle + |1\rangle)$$

|0> → Z → |0>

|1> → Z → -|1>

Flips the sign of 1

CNOT gate flips the target bit only if the control bit is 1.

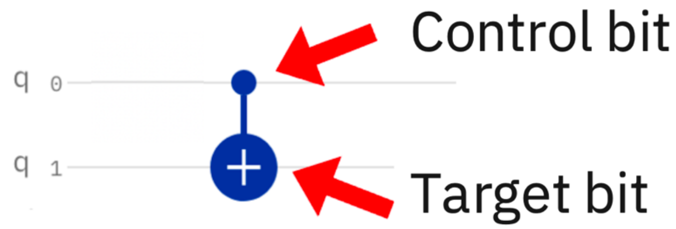

input		output	
Target bit	Control bit	Target bit	Control bit
0	0	0	0
1	0	1	0
0	1	**1**	**1**
1	1	**0**	**1**

$R_z(\theta)$

Measure Z basis

$e^{-i\theta Z\otimes Z/2}$

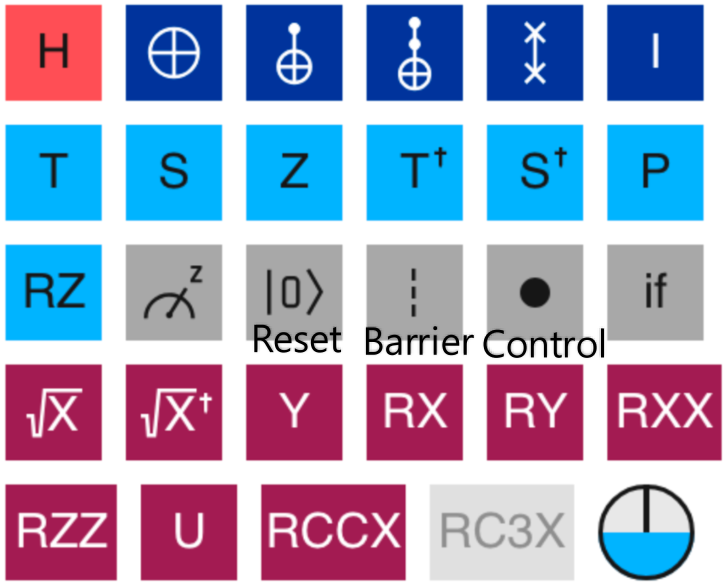

$$T = \begin{pmatrix} 1 & 0 \\ 0 & e^{i\pi/4} \end{pmatrix} \quad S = \begin{pmatrix} 1 & 0 \\ 0 & i \end{pmatrix} \quad P(\lambda) = \begin{pmatrix} 1 & 0 \\ 0 & e^{i\lambda} \end{pmatrix}$$

$$Y = \begin{pmatrix} 0 & -i \\ i & 0 \end{pmatrix} \quad R_{XX}(\theta) = e^{-i\theta X\otimes X/2}$$

$U(\theta, \phi, \lambda)$

RCCX (Relative-phase Toffoli)

RC3X (relative-phase 3-controlled X Gate)

Notation of multiple systems

- A one-qubit system can be in the superposition of two states:

$$|0\rangle\,,\quad |1\rangle$$

- A two-qubit system can be in the superposition of 2^2 states:

$$|0\rangle\otimes|0\rangle,\quad |1\rangle\otimes|0\rangle,\quad |0\rangle\otimes|1\rangle\,,\quad |1\rangle\otimes|1\rangle$$

$$\equiv\quad |0\rangle|0\rangle,\quad |1\rangle|0\rangle,\quad |0\rangle|1\rangle\,,\quad |1\rangle|1\rangle$$

$$\equiv\quad |00\rangle,\quad |10\rangle,\quad |01\rangle,\quad |11\rangle$$

- An n-qubit system can be in the superposition of 2^n states:

$$|0\rangle_{n-1}\otimes\cdots\otimes|0\rangle_0,\quad |0\rangle_{n-1}\otimes\cdots\otimes|0\rangle_1\otimes|1\rangle_0,\quad \cdots,\ |1\rangle_{n-1}\otimes\cdots\otimes|1\rangle_0$$

$$\equiv\quad |00\cdots0\rangle,\quad |0\cdots01\rangle,\quad \cdots,\ |1\cdots1\rangle$$

Tensor products

Tensor product of two vectors: multiply the right-hand vector by each component of the left-hand vector.

$$\begin{pmatrix} v_1 \\ \vdots \\ v_n \end{pmatrix} \otimes \begin{pmatrix} w_1 \\ \vdots \\ w_n \end{pmatrix} = \begin{pmatrix} v_1 \begin{pmatrix} w_1 \\ \vdots \\ w_n \end{pmatrix} \\ \vdots \\ v_n \begin{pmatrix} w_1 \\ \vdots \\ w_n \end{pmatrix} \end{pmatrix}$$

Tensor product of two matrices: multiply the right-hand matrix by each element of the left-hand matrix.

$$\mathrm{A} \otimes B = \begin{pmatrix} A_{11}B & A_{12}B \\ A_{21}B & A_{22}B \end{pmatrix} = \begin{pmatrix} A_{11}B_{11} & A_{11}B_{12} & A_{12}B_{11} & A_{12}B_{12} \\ A_{11}B_{21} & A_{11}B_{22} & A_{12}B_{21} & A_{12}B_{22} \\ A_{21}B_{11} & A_{21}B_{12} & A_{22}B_{11} & A_{22}B_{12} \\ A_{21}B_{21} & A_{21}B_{22} & A_{22}B_{21} & A_{22}B_{22} \end{pmatrix}$$

A two-qubit state can be represented as the tensor product of two single-qubit states.

$$|00\rangle = |0\rangle \otimes |0\rangle = \begin{pmatrix} 1 \\ 0 \end{pmatrix} \otimes \begin{pmatrix} 1 \\ 0 \end{pmatrix} = \begin{pmatrix} 1 \\ 0 \\ 0 \\ 0 \end{pmatrix} \equiv |0\rangle, \quad |01\rangle = |0\rangle \otimes |1\rangle = \begin{pmatrix} 1 \\ 0 \end{pmatrix} \otimes \begin{pmatrix} 0 \\ 1 \end{pmatrix} = \begin{pmatrix} 0 \\ 1 \\ 0 \\ 0 \end{pmatrix} \equiv |1\rangle,$$

$$|10\rangle = |1\rangle \otimes |0\rangle = \begin{pmatrix} 0 \\ 1 \end{pmatrix} \otimes \begin{pmatrix} 1 \\ 0 \end{pmatrix} = \begin{pmatrix} 0 \\ 0 \\ 1 \\ 0 \end{pmatrix} \equiv |2\rangle, \quad |11\rangle = |1\rangle \otimes |1\rangle = \begin{pmatrix} 0 \\ 1 \end{pmatrix} \otimes \begin{pmatrix} 0 \\ 1 \end{pmatrix} = \begin{pmatrix} 0 \\ 0 \\ 0 \\ 1 \end{pmatrix} \equiv |3\rangle$$

Entangled state

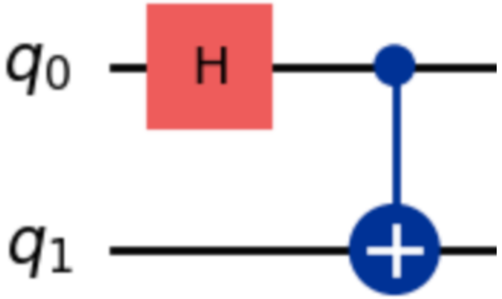

$$|0\rangle_1 \otimes |0\rangle_0 \xrightarrow[I\otimes H]{} |0\rangle \otimes \frac{1}{\sqrt{2}}(|0\rangle + |1\rangle)$$

$$= \frac{1}{\sqrt{2}}(|00\rangle + |01\rangle)$$

$$\xrightarrow[CNOT]{} \frac{1}{\sqrt{2}}(|00\rangle + |11\rangle)$$

An entangled state is a state $|\psi\rangle_{AB}$ consisting of quantum states $|\psi\rangle_A$ and $|\psi\rangle_{\mathrm{B}}$ that cannot be represented by a tensor product of individual quantum states.

$$\frac{1}{\sqrt{2}}(|00\rangle + |11\rangle) \neq (a_0|0\rangle + a_1|1\rangle)\otimes(b_0|0\rangle + b_1|1\rangle)$$

$$= a_0 b_0|00\rangle + a_1 b_0|10\rangle + a_0 b_1|01\rangle + a_1 b_1|11\rangle$$

There is no coefficient which satisfies this equation. Therefore, this state is entangled state.

Quantum Circuit: Bell States

$$|\Phi^+\rangle = \frac{1}{\sqrt{2}}(|00\rangle + |11\rangle)$$

$$|\Phi^-\rangle = \frac{1}{\sqrt{2}}(|00\rangle - |11\rangle)$$

$$|\Psi^+\rangle = \frac{1}{\sqrt{2}}(|01\rangle + |10\rangle)$$

$$|\Psi^-\rangle = \frac{1}{\sqrt{2}}(|01\rangle - |10\rangle)$$

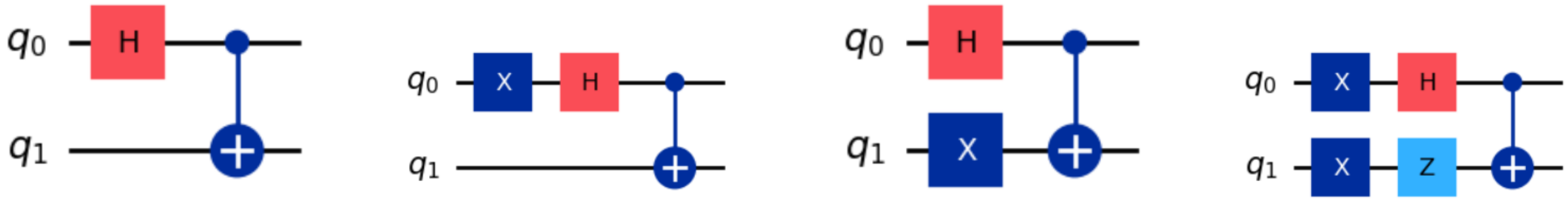

(a) $|\Phi^+\rangle$ state (b) $|\Phi^-\rangle$ state (c) $|\Psi^+\rangle$ state (d) $|\Psi^-\rangle$ state

Figure 8: Quantum circuits used to create the four Bell states: $|\Phi^+\rangle$, $|\Phi^-\rangle$, $|\Psi^+\rangle$, and $|\Psi^-\rangle$. Each circuit applies a combination of Hadamard, CNOT, Pauli-X, and Pauli-Z gates to two qubits (q_0 and q_1), producing maximally entangled states.

Quantum Circuit: GHZ states (Greenberger-Horne-Zeilinger states)

$$|\mathrm{GHZ}\rangle = \frac{1}{\sqrt{2}}\left(|0000\rangle + |1111\rangle\right)$$

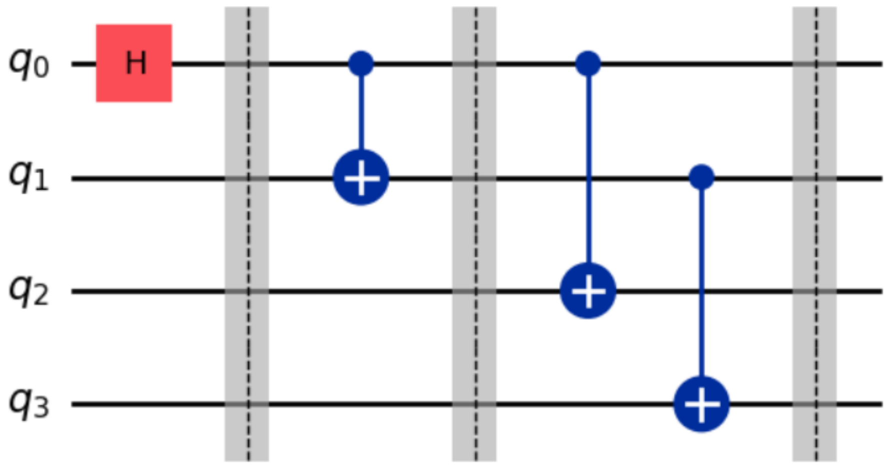

Figure 10: Quantum circuit for preparing a 4-qubit GHZ state. The circuit starts with a Hadamard gate applied to the first qubit, followed by two layers of CNOT gates that entangle all four qubits, creating a maximally entangled GHZ state. The three gray vertical dashed lines represent barriers, showing that this quantum circuit consists of three layers.

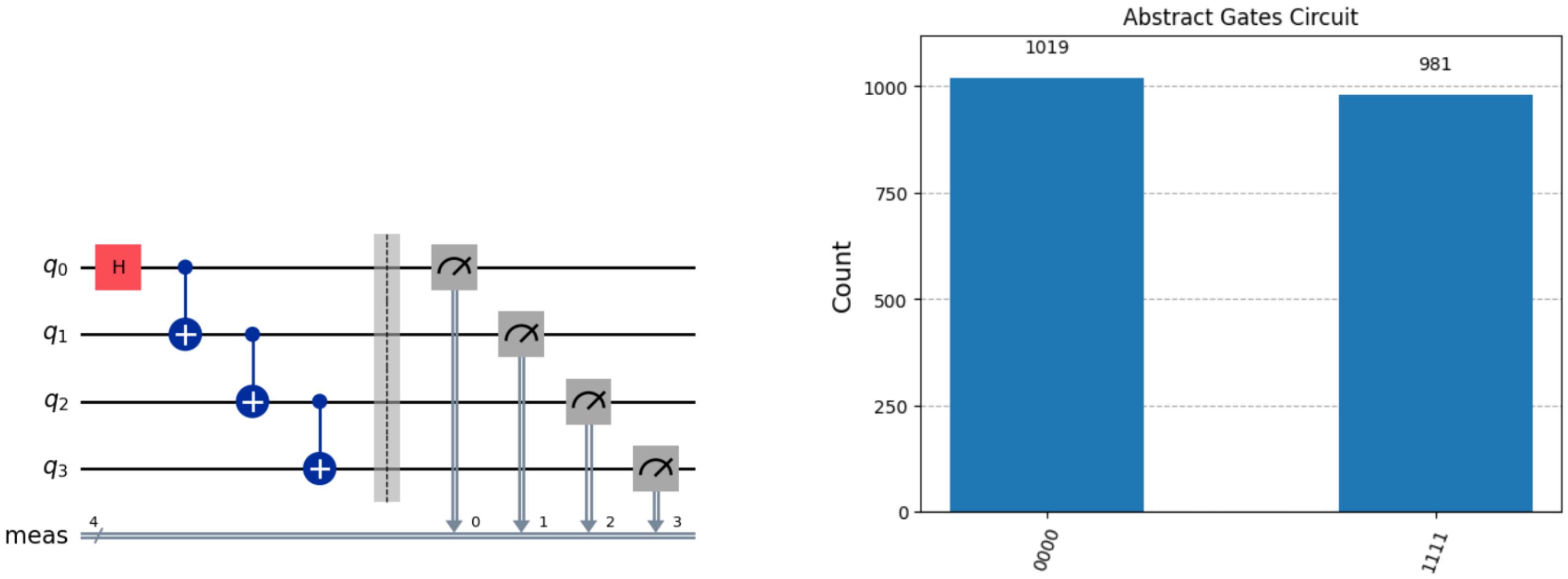

(a) Abstract gates circuit and measurement results

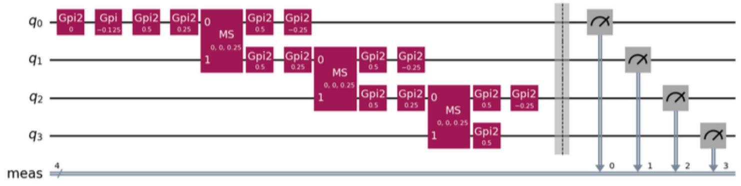

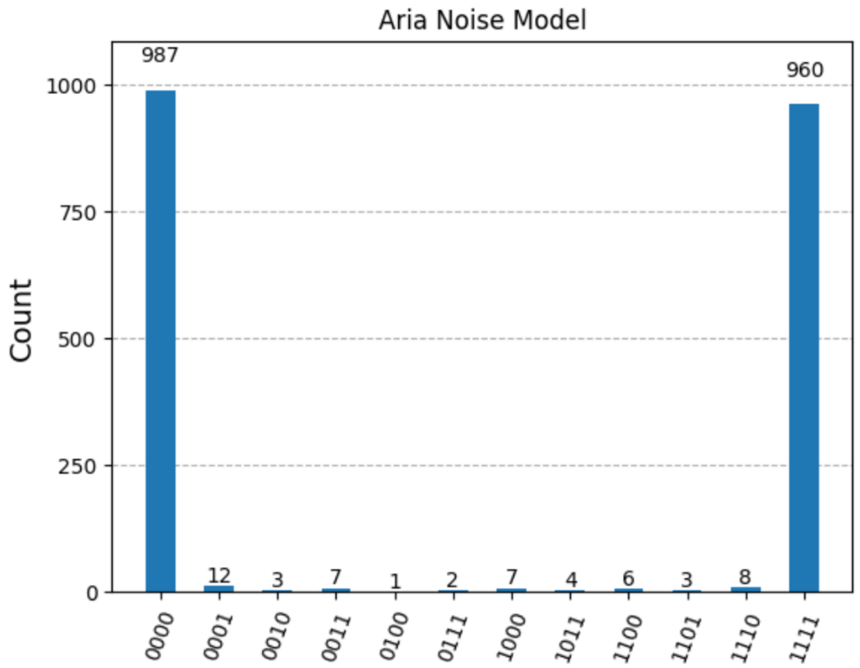

(b) Transpilied gates circuit and

Variational Quantum Eigensolver (VQE)

Variational Quantum Eigensolver

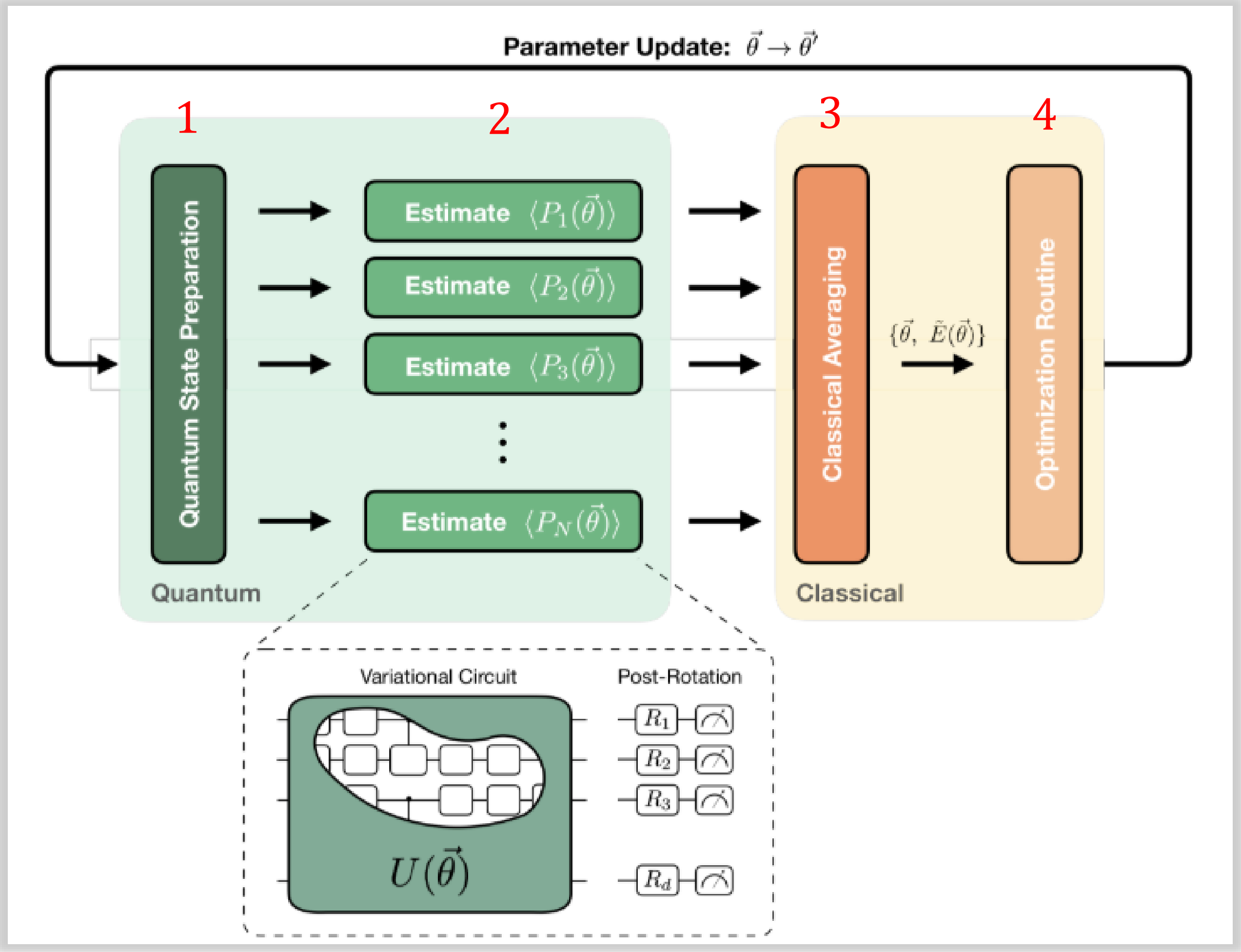

- Ground state energy estimation

1. Prepare quantum state(Ansatz)
2. Measure energy
3. Classical averaging
4. Optimization(Classical) → Parameter update

*** Ansatz

Unitary Coupled Cluster(UCC) method

$$|\psi(\theta)\rangle = U(\theta)|\psi_0\rangle = e^{T-T^{+}}|\Psi_0\rangle \quad \text{where } T = \sum_i T_i$$

$$T_1 = \sum t_{i\alpha} a_i^{+} a_i \ \ \& \ \ T_2 = \sum t_{ij\alpha\beta} a_i^{+} a_j^{+} a_\alpha a_\beta$$

arXiv:1812.09976v2

Deuteron

B. Deuteron model

p n

⟨Deuteron⟩

$M_p = 938.3 \mathrm{MeV}/c^2$ & $M_n = 939.6 \mathrm{MeV}/c^2$ & $\kappa = 0.67$ & $r_0 = 1.27 \mathrm{fm}$ & $a_0 = 0.67 \mathrm{fm}$

& $\lambda = 32 \mathrm{fm}^{-1}$ & $M = \frac{M_p + M_n}{2} = 938.95 \mathrm{MeV}/c^2$

Nuclear interaction btw proton & neutron

$$\rightarrow H = \sum_{i=1}^{Z} \frac{p_i{}^2}{2M_p} + \sum_{i=Z+1}^{A} \frac{p_j{}^2}{2M_n} + \sum_{k=1}^{A} V(r_k) + \cancel{\sum_{1 \le i_1 \le i_2 \le Z} \frac{e^2}{4\pi\epsilon_0} \frac{1}{|r_{i_1} - r_{i_2}|}} + \cancel{\frac{1}{2} \sum_{k_1 \neq k_2} v(k_1, k_2)}$$

proton $\rightarrow \{\psi_{\pi,i}\}_{i=1}^{N_\pi}$

neutron $\rightarrow \{\psi_{\upsilon,j}\}_{j=1}^{N_\upsilon}$

Kinetic Energy of proton

Kinetic Energy of neutron

$$\rightarrow V(\mathbf{r}) = U_c(r) - 2\lambda \frac{\hbar}{2Mc}^2 \cdot \frac{dU_c(r)}{dr} \mathbf{s} \cdot \mathbf{l} \quad \& \quad U_c(r) = \frac{U_0 \left(1 \pm \cancel{\kappa \frac{N - Z}{N + Z}}\right)}{1 + \exp\left(\frac{r - r_0 A^{\frac{1}{3}}}{a_0}\right)} \rightarrow \text{wood saxon potential}$$

B. Deuteron model

$$\rightarrow H = \sum_{\alpha'}\sum_{\alpha} \underline{g_\pi(\alpha',\alpha)} a^+_{\pi,\alpha'} a_{\pi,\alpha} \otimes I_\nu + \cancel{\sum_{\alpha_1'\alpha_2'}\sum_{\alpha_1\alpha_2} \underline{h_\pi(\alpha_1',\alpha_2',\alpha_1,\alpha_2)} a^+_{\pi,\alpha_1'} a^+_{\pi,\alpha_2'} a_{\pi,\alpha_2} a_{\pi,\alpha_1} \otimes I_\nu}$$

$$+ \sum_{\beta'}\sum_{\beta} \underline{g_\nu(\beta',\beta)} I_\pi \otimes a^+_{\nu,\beta'} a_{\nu,\beta} + \cancel{\sum_{\beta_1'\beta_2'}\sum_{\beta_1\beta_2} \underline{h_\nu(\beta_1',\beta_2',\beta_1,\beta_2)} I_\pi \otimes a^+_{\nu,\beta_1'} a^+_{\nu,\beta_2'} a_{\nu,\beta_2} a_{\nu,\beta_1}}$$

$$\cancel{+ \sum_{\alpha'\beta'}\sum_{\alpha\beta} \underline{h_{\pi\nu}(\alpha',\alpha,\beta',\beta)} a^+_{\pi,\alpha'} a_{\pi,\alpha} \otimes a^+_{\nu,\beta'} a_{\nu,\beta}}$$

$\alpha, \alpha', \alpha_1, \alpha_1', \alpha_2, \alpha_2' \in \{1,2,\ldots,N_\pi\}$

$\beta, \beta', \beta_1, \beta_1', \beta_2, \beta_2' \in \{1,2,\ldots,N_\nu\}$

$$* \ \underline{g_\pi(\alpha',\alpha)} = \left\langle \psi_{\pi,\alpha'} \middle| \frac{p^2}{2M_p} + V(r) \middle| \psi_{\pi,\alpha'} \right\rangle \ \& \ \underline{g_\nu(\beta',\beta)} = \left\langle \psi_{\nu,\beta'} \middle| \frac{p^2}{2M_n} + V(r) \middle| \psi_{\nu,\beta'} \right\rangle$$

$$\underline{h_\pi(\alpha_1',\alpha_2',\alpha_1,\alpha_2)} = \left\langle \psi_{\pi,\alpha_1'} \middle| \left\langle \psi_{\pi,\alpha_2'} \middle| \frac{1}{2}\left\{ \frac{e^2}{4\pi\epsilon_0}\frac{1}{|r_{i_1} - r_{i_2}|} + v(\pi_1,\pi_2) \right\} \middle| \psi_{\pi,\alpha_1} \right\rangle \middle| \psi_{\pi,\alpha_2} \right\rangle$$

$$\underline{h_\nu(\beta_1',\beta_2',\beta_1,\beta_2)} = \left\langle \psi_{\nu,\beta_1'} \middle| \left\langle \psi_{\nu,\beta_2'} \middle| \frac{1}{2} v(\nu_1,\nu_2) \middle| \psi_{\pi,\beta_1} \right\rangle \middle| \psi_{\pi,\beta_2} \right\rangle \quad \& \quad \underline{h_{\pi\nu}(\alpha',\alpha,\beta',\beta)} = \langle \psi_{\pi,\alpha'} | \langle \psi_{\upsilon,\beta'} | v(\pi,\nu) | \psi_{\pi,\alpha} \rangle | \psi_{\nu,\beta} \rangle$$

QCSH: A full quantum computer nuclear shell-model package | Science China Physics, Mechanics &

B. Deuteron model

$$\rightarrow H_N = \sum_{n,n'=0}^{N-1} \langle n'|T+V|n\rangle a_{n'}^{\dagger} a_n$$

$$\langle n'|T|n\rangle = \frac{\hbar w}{2}\left[\left(2n+\frac{3}{2}\right)\delta_n^{n'} - \sqrt{n\left(n+\frac{1}{2}\right)}\,\delta_n^{n'+1} - \sqrt{(n+1)\left(n+\frac{3}{2}\right)}\,\delta_n^{n'-1}\right] \ \& \ \langle n'|V|n\rangle = V_0\delta_n^0\delta_n^{n'}$$

→ Jordan – Wigner transformation method

$$a_n^{\dagger} \rightarrow \frac{1}{2}\left[\prod_{j=0}^{n-1} -Z_j\right](X_n - iY_n),$$

$$a_n \rightarrow \frac{1}{2}\left[\prod_{j=0}^{n-1} -Z_j\right](X_n + iY_n).$$

$$H_2 = 5.906709 I + 0.218291 Z_0 - 6.125 Z_1 - 2.143304\,(X_0X_1 + Y_0Y_1)\,.$$

$$\sigma_x^i \rightarrow \frac{1-\sigma_z^{ij}\sigma_z^{ik}}{2}S(j)S(k) \qquad \sigma_y^i \rightarrow i\frac{\sigma_z^{ik}-\sigma_z^{ij}}{2}S(j)S(k)$$

$$\sigma_z^i \rightarrow \frac{\sigma_z^{ij}+\sigma_z^{ik}}{2}S(j)S(k) \qquad \mathbb{1} \rightarrow \frac{1+\sigma_z^{ij}\sigma_z^{ik}}{2}S(j)S(k)$$

B. Deuteron model

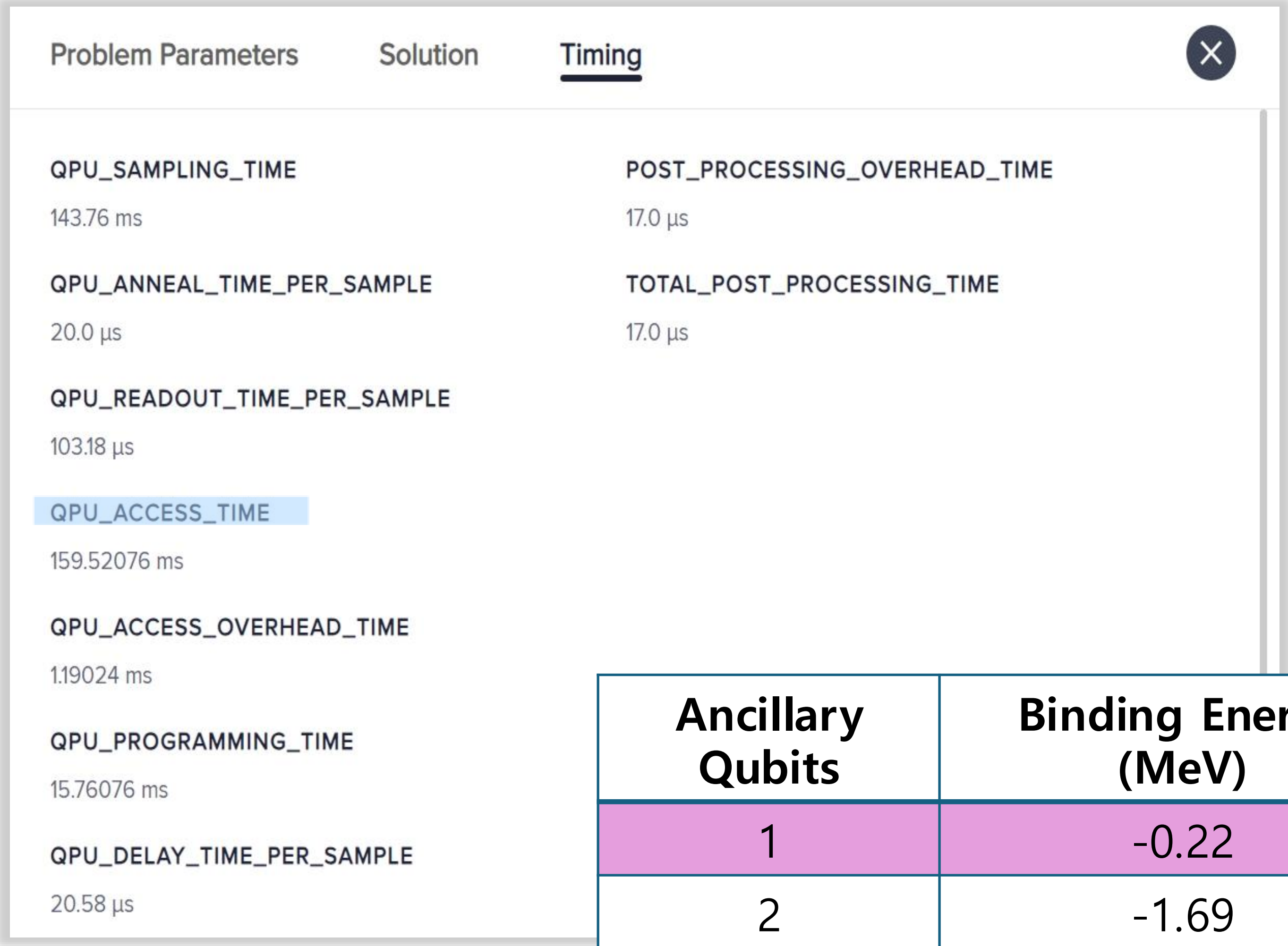

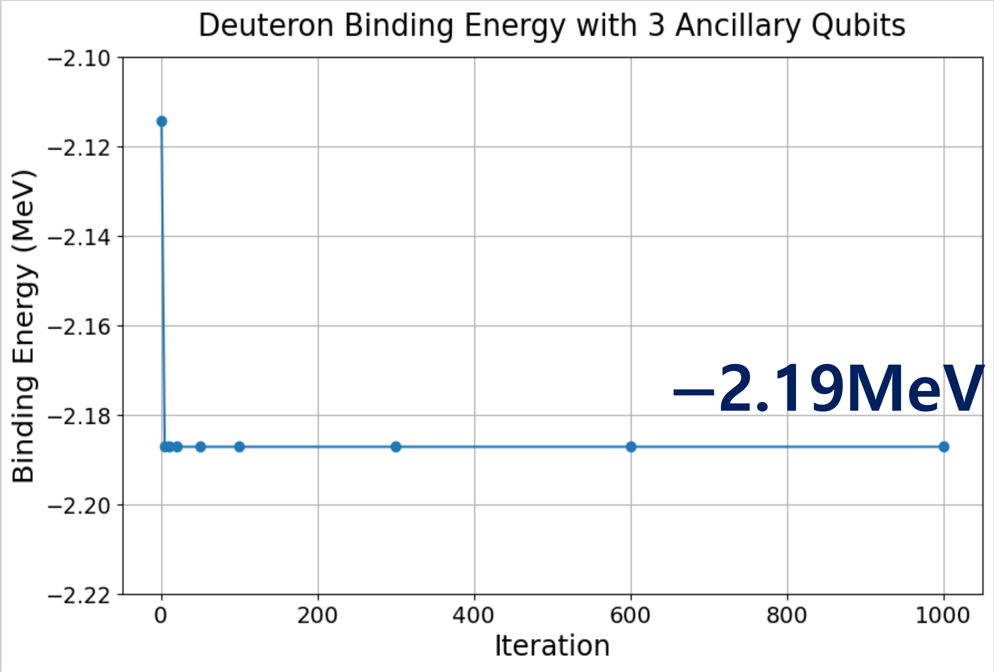

Ancillary Qubits	Binding Energy (MeV)	QPU Access Time (ms)
1	-0.22	79.76
2	-1.69	122.2
3	-2.19	159.5

1.Dumitrescu, McCaskey, et al., **PRL 120, 210501 (2018)**
“Cloud Quantum Computing of an Atomic Nucleus”
2.Lu, Ekström, et al., **PRC 103, 024310 (2021)**
“Simulations of the deuteron on a trapped-ion quantum computer”

(1) 가장 많이 사용된 양자컴 기반 Deuteron (^{2}H) — Hamiltonian

•A well-established 2-qubit effective Hamiltonian for the deuteron ground state derived from the LO pionless EFT in a truncated harmonic-oscillator basis.

•The Hamiltonian is written in the Pauli-operator form:

$$H_1 = 0.218291(Z_0 - I_0)$$

$$H_2 = 5.906709 I_1 \otimes I_0 + 0.218291 I_1 \otimes Z_0 - 6.215 Z_1 \otimes I_0 - 2.143304(X_1 \otimes X_0 + Y_1 \otimes Y_0)$$

$$H_3 = I_2 \otimes H_2 + 9.625(I_2 \otimes I_1 \otimes I_0 - Z_2 \otimes I_1 \otimes I_0) - 3.913119(X_2 \otimes X_1 \otimes I_0 + Y_2 \otimes Y_1 \otimes I_0)$$

•This Hamiltonian corresponds to a **two-state truncation (N=2)** of the deuteron S-wave sector.

< Low-depth circuits for the ansatz >

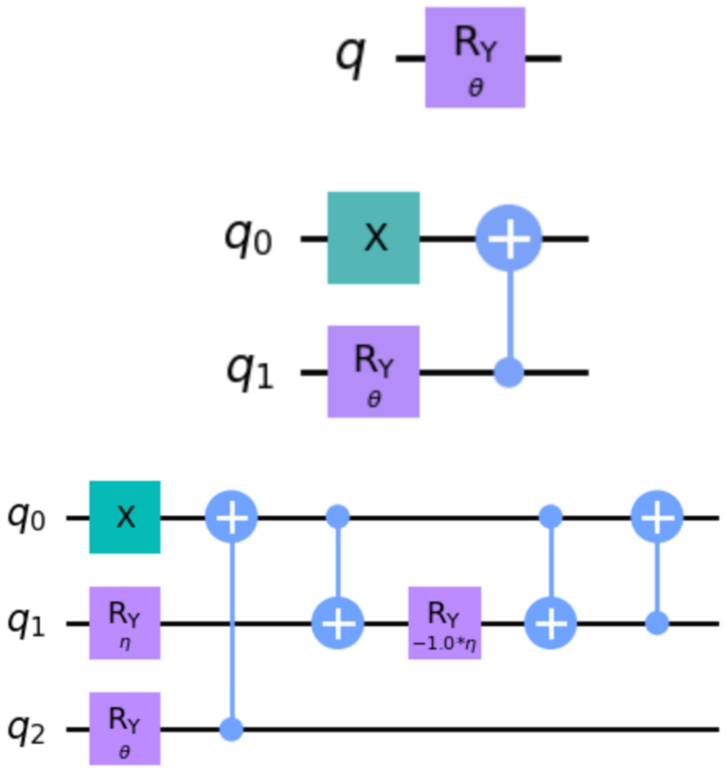

특징:

이 Hamiltonian은 다음을 포함한다:
- LO EFT에서 나오는 **S-wave + D-wave 혼합 구조**
- deuteron이 실제로 갖는 **텐서력에 의한 D-state admixture**
- 상대좌표 + 스핀-아이소스핀 자유도 일부를 포함한 **4차원 모델공간**

따라서 **2개의 논리 큐비트 필요**

(2) Deuteron Hamiltonian (2×2 형태, 1qubit)

특정 규격화 후 가장 흔히 사용되는 수치: $H_d = \begin{pmatrix} -1.7492 & -0.4330 \\ -0.4330 & -0.6443 \end{pmatrix}$ MeV

- 1 qubit 으로 표현 가능한 최소 모델
- Pauli 연산자로 분해 가능: $H = c_0 I + c_x X + c_z Z$
- VQE 데모에 가장 적합한 Hamiltonian

특징:

- 상대좌표 HO 기저 |0s>, |1s> **단 두 개만 남긴 모델**
- D-wave는 아예 제거됨.
- spin/isospin 자유도도 완전히 평균화된 상태
- EFT 또는 HO basis에서 나온 더 큰 Hamiltonian을
그냥 2차원 subspace로 projection/downfold 한 것.

https://qiskit-community.github.io/qiskit-nature/tutorials/12_deuteron_binding_energy.html

VQE Result (H_2) for the Deuteron Ground State

- VQE optimization performed using COBYLA
- Backend: **Statevector**
- Final energy: $E_{\text{VQE}} = -1.748865\ MeV$
- Reference value: $E_{\text{ref}} = -1.748860\ MeV$
- Absolute error:
- $|\ E - E_{\text{ref}}\ | = 4.7 \times 10^{-6}$

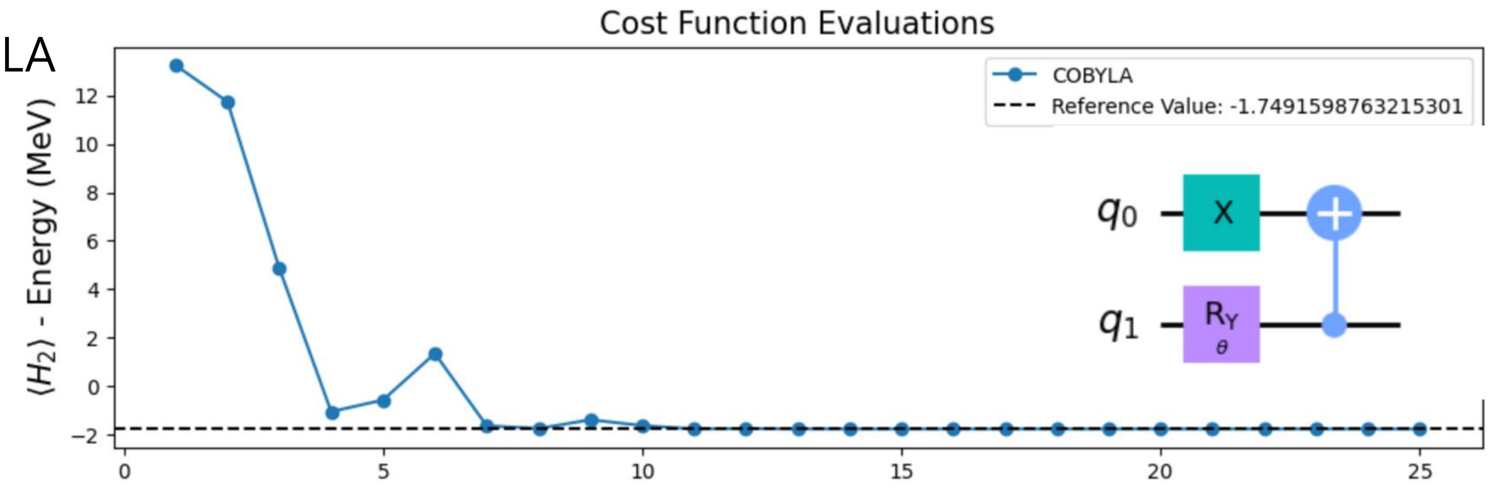

COBYLA — Constrained Optimization BY Linear Approximations
(Gradient- and Derivative-free optimizer)

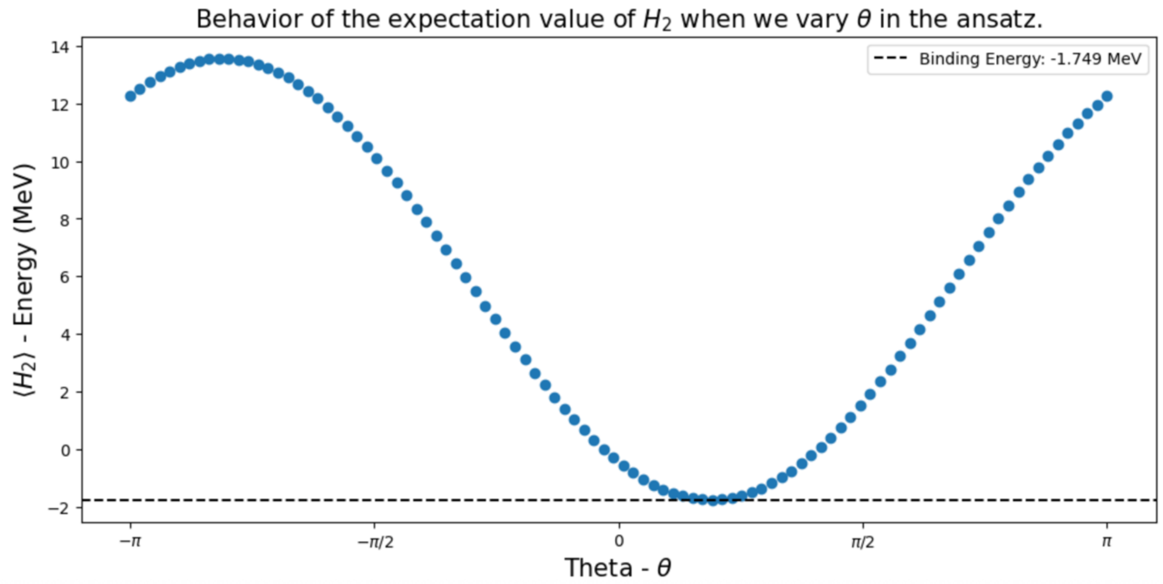

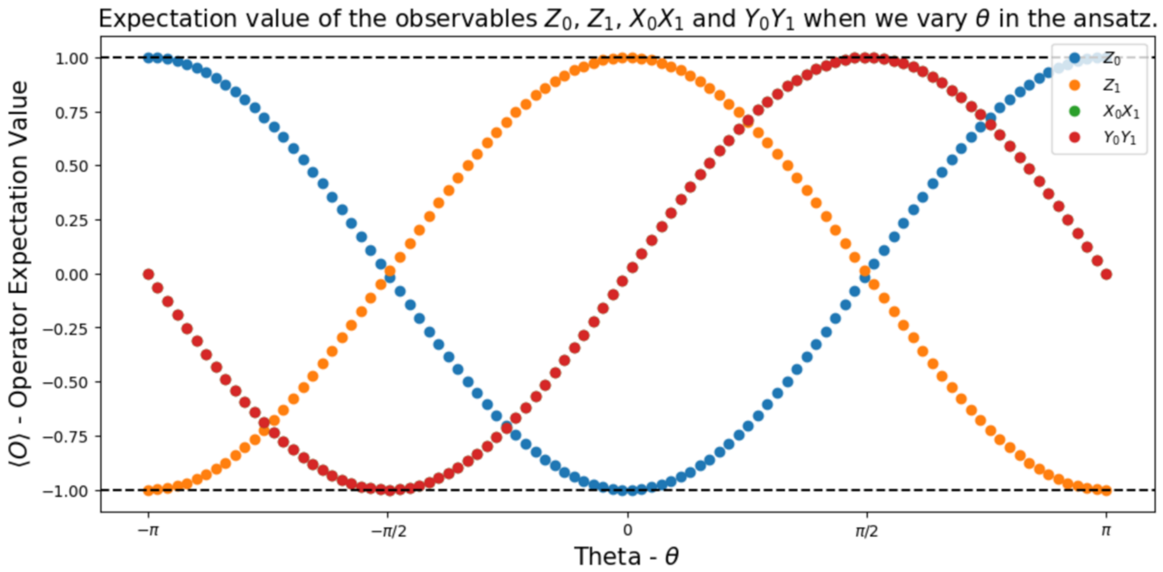

VQE Result (H_3) for the Deuteron Ground State

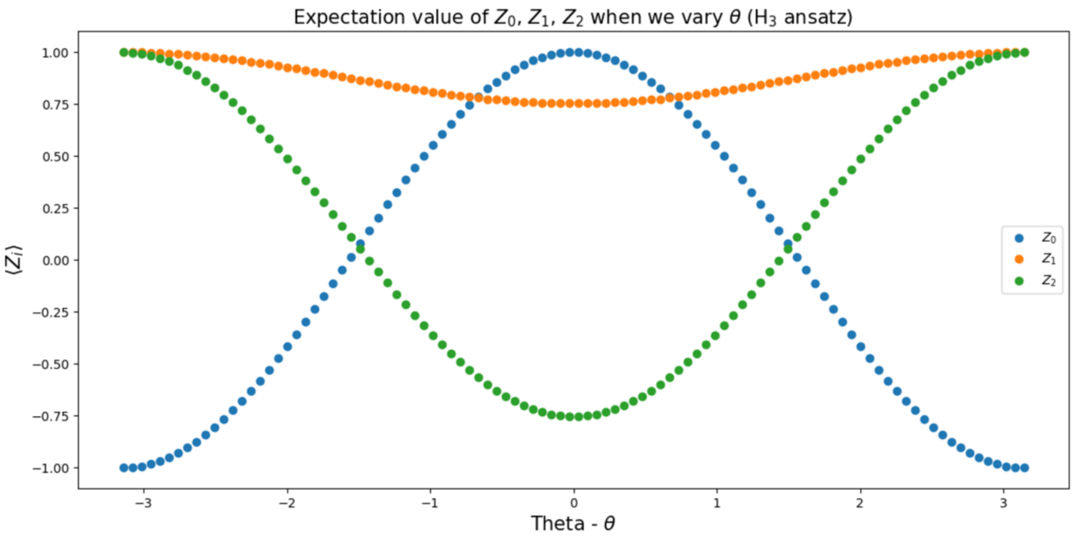

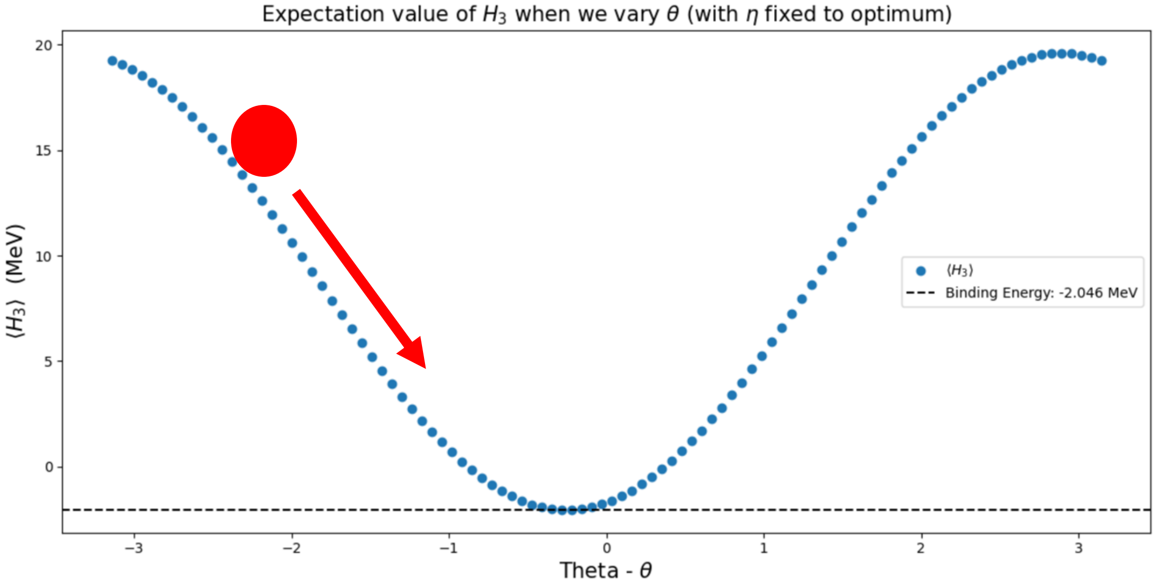

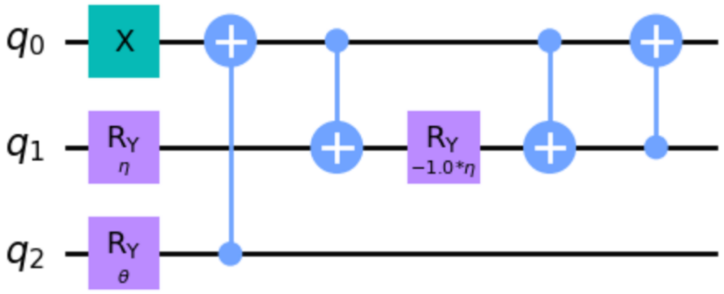


```
Results using Estimator for H_1, H_2, H_3 and H_4

Binding energy for H_1: -0.43658065601609036 MeV
Binding energy for H_2: -1.7491598672779776 MeV
Binding energy for H_3: -2.0456704129777483 MeV
Binding energy for H_4: -2.1439230360569255 MeV
```

하지만, 실제 양자컴에서는.....

※ 노이즈가 들어오면 landscape에 “작은 우물”들이 생긴다

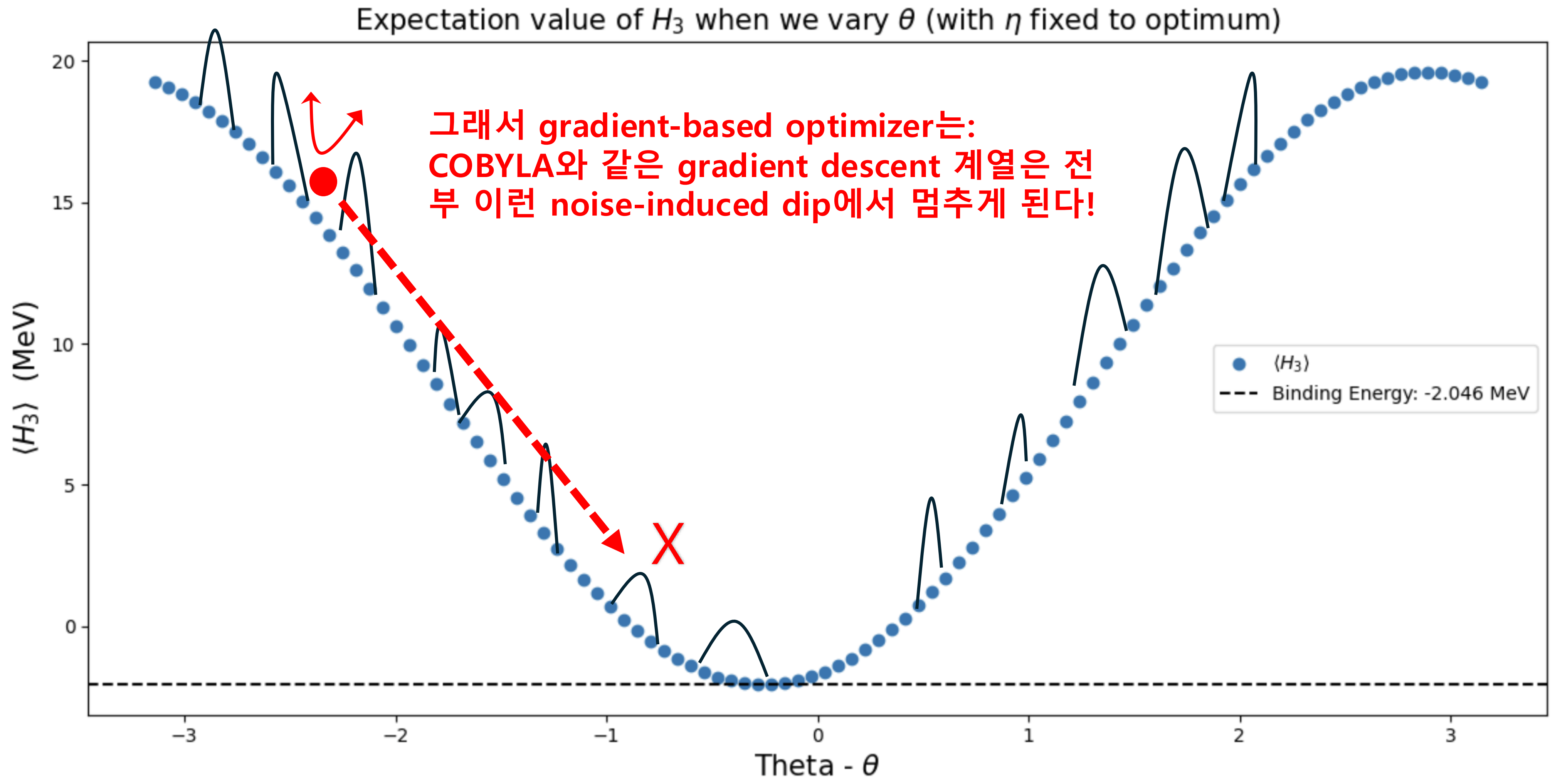

※ **반복하면 할수록 dip가 더 많이 생긴다 : 1.** 노이즈는 반복할수록 누적, 2. decoherence는 depth에 비례해서 증가, 3. drift 때문에 landscape 자체가 매 iteration 조금씩 변함

따라서 optimizer가 실행되는 동안:1. landscape 변함, 2 더 많은 dip 생김 optimizer는 계속 새로운 dip에 갇힘

결과적으로: **반복하면 할수록 global minimum은 멀어질 수 있다.**

※ 2018년에서 2025년까지 하드웨어 성능의 향상

항목	2018–2020 IBM Q (5–20 qubits)	2023–2025 IBM Heron (133 qubits)	개선 여부	VQE 결과에 대한 영향
T_1 (s)	50–80 μs	200–320 μs	**4배 향상**	ansatz 유지 시간 ↑ → decoherence 감소 (부분 개선)
T_2 (s)	40–70 μs	250–450 μs	**5–6배 향상**	coherence boost → shallow circuit 안정성 향상
1-qubit gate fidelity	99.0–99.5%	99.99% (10^{-4} error)	**10배 개선**	단일 큐비트 회로는 매우 안정적
2-qubit gate fidelity	97–99%	99.5–99.8%	**10–30배 개선**	entanglement rotation이 안정 → ansatz 품질 개선
Readout error	3–8%	0.2–0.7%	**10–30배 개선**	SPAM 노이즈가 크게 줄어 듦
Gate depth 허용도	depth > 30이면 거의 완전 decoherence	depth 200~300까지 안정적으로 유지	**6–10배↑**	shallow ansatz는 성공률 증가
Cross-talk	상당히 심함	매우 낮음 (heron layout 개선)	개선	multi-qubit correlation 안정
Calibration drift	매우 심함 (시간당 수% 변화)	훨씬 안정 (시간당 <1%)	개선	energy landscape drift 감소
Effective noise model	depolarizing + thermal + readout 혼합	depolarizing dominance + SPAM suppression	개선중	noise-induced dip는 줄었지만 완전히 사라지지 않음
VQE global minimum 접근	거의 불가능	가능성이 약간 증가	(일부 개선)	여전히 noise-induced dips 때문에 어려움
Noise-induced fake minima	landscape에 다수 존재	수는 줄었지만 여전히 존재	△ (부분적 개선)	**VQE 실패 원인 여전**
Large-scale chemistry	완전 불가능	error mitigation과 결합 시 “가능성은 있음”	실패	하지만 해밀토니안 큰 경우 여전히 실패
IBM 공식 견해(2024)	VQE 연구 초기 단계	“VQE는 scaling이 어려움. 목적 특화 알고리즘으로 전환 필요”	→	Officially: **General VQE는 한계 명확**

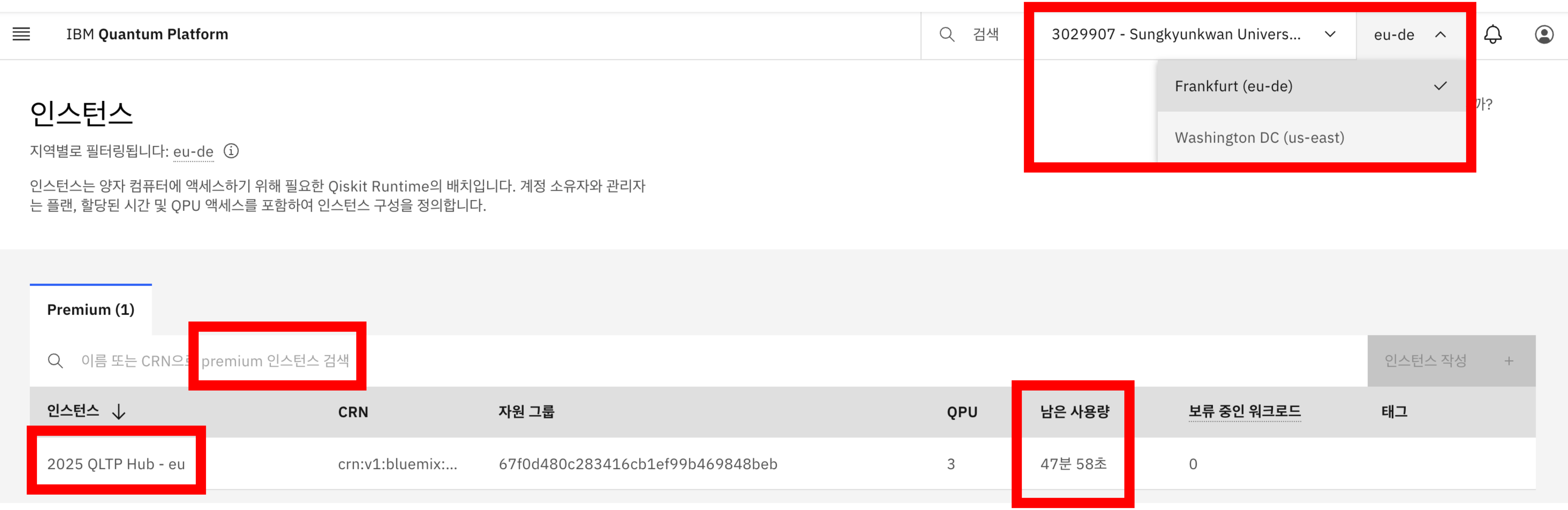
IBM Quantum Platform
검색
3029907 - Sungkyunkwan Univers...
eu-de
Frankfurt (eu-de)
Washington DC (us-east)
인스턴스
지역별로 필터링됩니다: eu-de
인스턴스는 양자 컴퓨터에 액세스하기 위해 필요한 Qiskit Runtime의 배치입니다. 계정 소유자와 관리자는 플랜, 할당된 시간 및 QPU 액세스를 포함하여 인스턴스 구성을 정의합니다.
Premium (1)
premium 인스턴스 검색
인스턴스 작성
인스턴스
CRN
자원 그룹
QPU
남은 사용량
보류 중인 워크로드
태그
2025 QLTP Hub - eu
crn:v1:bluemix:...
67f0d480c283416cb1ef99b469848beb
3
47분 58초
0

ID 또는 태그로 검색

내 워크로드 ✕ 필터 재설정

ID	상태	인스턴스	모드	작성일시	완료됨	QPU	사용량	사용자	태그
d4fa811f7ups7...	완료됨	2025 QLTP Hub - eu	작업	25. 11. 20. 오후 2:15	25. 11. 20. 오후 2:16	ibm_aachen	53초	Jubin Park	
d4fa7gjp297s7...	완료됨	2025 QLTP Hub - eu	작업	25. 11. 20. 오후 2:14	25. 11. 20. 오후 2:15	ibm_aachen	52초	Jubin Park	
d4fa6ghf7ups7...	완료됨	2025 QLTP Hub - eu	작업	25. 11. 20. 오후 2:12	25. 11. 20. 오후 2:13	ibm_aachen	24초	Jubin Park	
d4fa688s84uc7...	완료됨	2025 QLTP Hub - eu	작업	25. 11. 20. 오후 2:12	25. 11. 20. 오후 2:12	ibm_aachen	24초	Jubin Park	
d4f9s1v6qdos7...	완료됨	2025 QLTP Hub - eu	작업	25. 11. 20. 오후 1:50	25. 11. 20. 오후 1:50	ibm_aachen	15초	Jubin Park	
d4f9rsf6qdos73...	완료됨	2025 QLTP Hub - eu	작업	25. 11. 20. 오후 1:49	25. 11. 20. 오후 1:50	ibm_aachen	14초	Jubin Park	
d4f9pdos84uc7...	완료됨	2025 QLTP Hub - eu	작업	25. 11. 20. 오후 1:44	25. 11. 20. 오후 1:44	ibm_aachen	14초	Jubin Park	
d4f9p70s84uc7...	완료됨	2025 QLTP Hub - eu	작업	25. 11. 20. 오후 1:44	25. 11. 20. 오후 1:44	ibm_aachen	20초	Jubin Park	

페이지당 항목 수 10 | 8개 항목 | 1개의 페이지

IBM **Quantum Platform**

검색

3029907 - Sungkyunkwan Univers...

eu-de

모든 워크로드 /

d4fa811f7ups73d550c0

조치

세부사항

태그 편집

사용자
Jubin Park

인스턴스
2025 QLTP Hub - eu

양자 컴퓨터
ibm_aachen

지역
Frankfurt (eu-de)

모드
작업

프로그램
estimator

PUB 수
100

태그

상태 세부사항

상태
완료됨

사용량 통계

실제 QR 사용량
53초

상태 타임라인

- 작성일시: 2025. 11. 20. 오후 2:15
- 보류 중: 0초
- 진행 중: 2025. 11. 20. 오후 2:15
  Qiskit Runtime 사용법: 53초
- 완료됨: 2025. 11. 20. 오후 2:16

총 완료 시간: 1분 4초

1 100개 회로 중

다이어그램 | Qasm | Qiskit

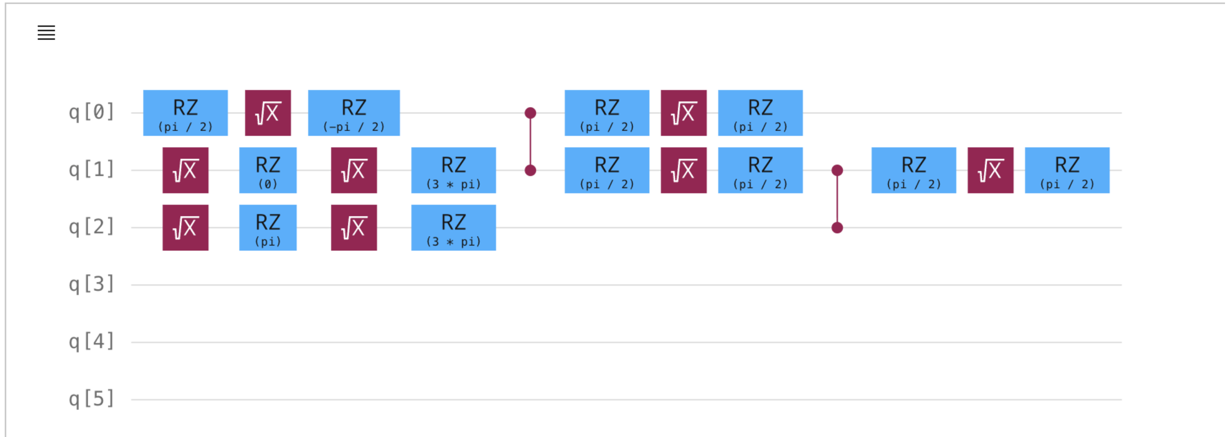

실제 양자컴 결과

Gate Depth ↑

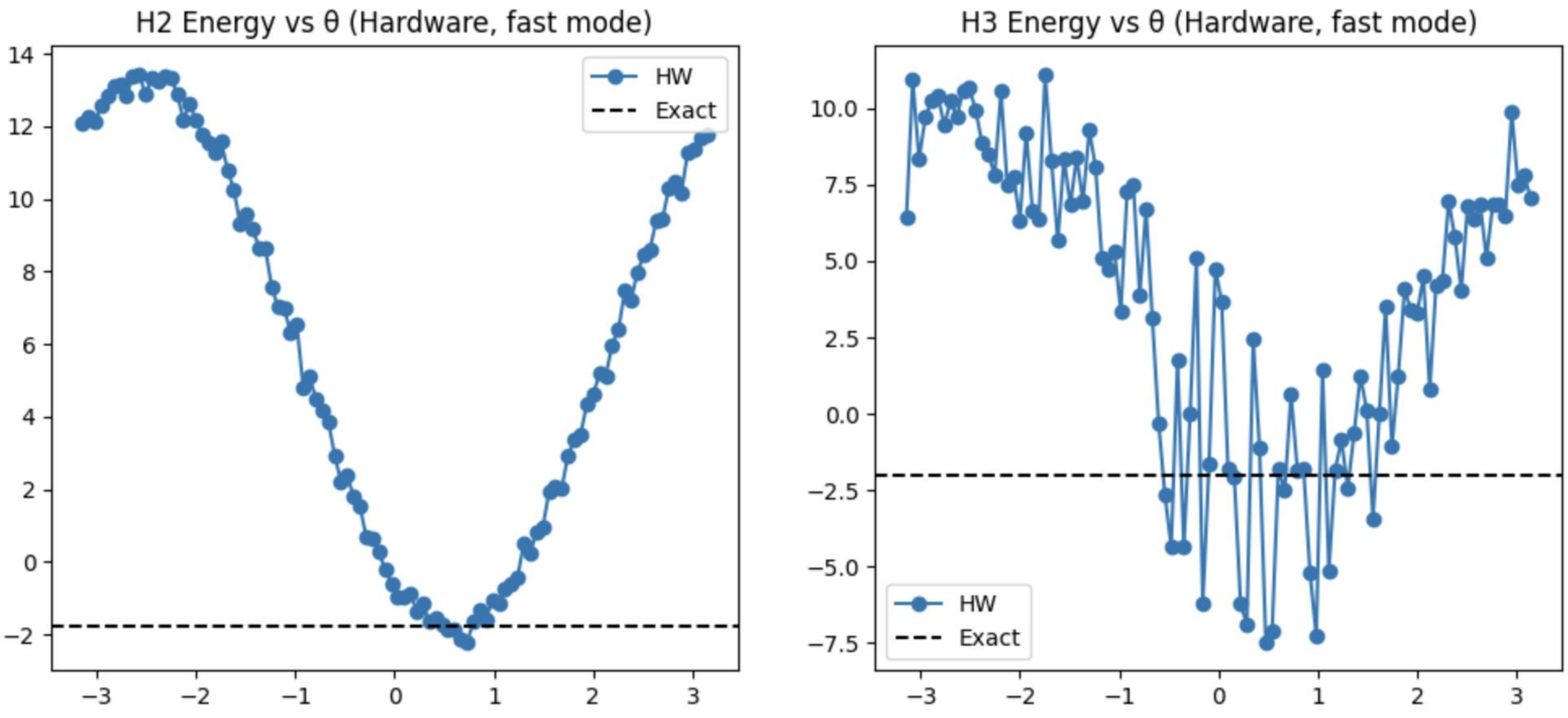

Conclusions — IBM Quantum

- IBM의 최신 Heron/Nighthawk 아키텍처는
  T_1/T_2, 2-qubit gate fidelity, readout error가 비약적으로 향상됨.

- 그러나 **VQE는 여전히 NISQ에서 근본적 한계**를 보임:
  - noise-induced local minima (“fake minima”)가 landscape에 다수 생성
    반복할수록 dip 증가 → optimizer(COBYLA 등)가 계속 잘못된 우물에 갇힘
  - 실제 디바이스에서는 **global minimum 접근이 거의 불가능**

- 1–2 qubit 수준의 간단한 해밀토니안(H_2, H_3, H_4)은
  statevector/backends에서는 정확히 재현,
  하지만 **실제 양자컴에서는 optimal solution까지 수렴 실패**.

- **→ IBM Q 기반 VQE는 ‘아주 작은 모델’에서는 가능하나,**
  noise 작용 때문에 실 디바이스에서의 확장성(scalability)은 여전히 제한적.

Possible Outlook

- IBM Nighthawk + error-mitigation 결합 시
  소규모 핵계(n≤3–4)에는 도전 가능성이 있음!
- Deuteron 이상의 핵계
  → VQE보다는 목적특화 알고리즘이 필요

- 반면, D-Wave는
  – 어닐링을 통한 핵의 바닥상태에너지를 찾는데 성공적이었음!
  – 클러스터 연구, 핵구조 최적화(예: configuration mixing)에 적용 가능

Thank you for your attention!

Backup Slides

taken from Dr. **Scott N. Genin**'s presentation

Variational Quantum Eigensolver

$\hat{H} = \sum \hat{P}_i$ Where $\hat{P}_i = \prod \sigma_j^n$, n = {x,y,z} & j = qubit index

$E_0 \leq \sum \langle \Psi_i | \hat{P}_i | \Psi_i \rangle$ Where Ψ is wavefunction of the ith Pauli word

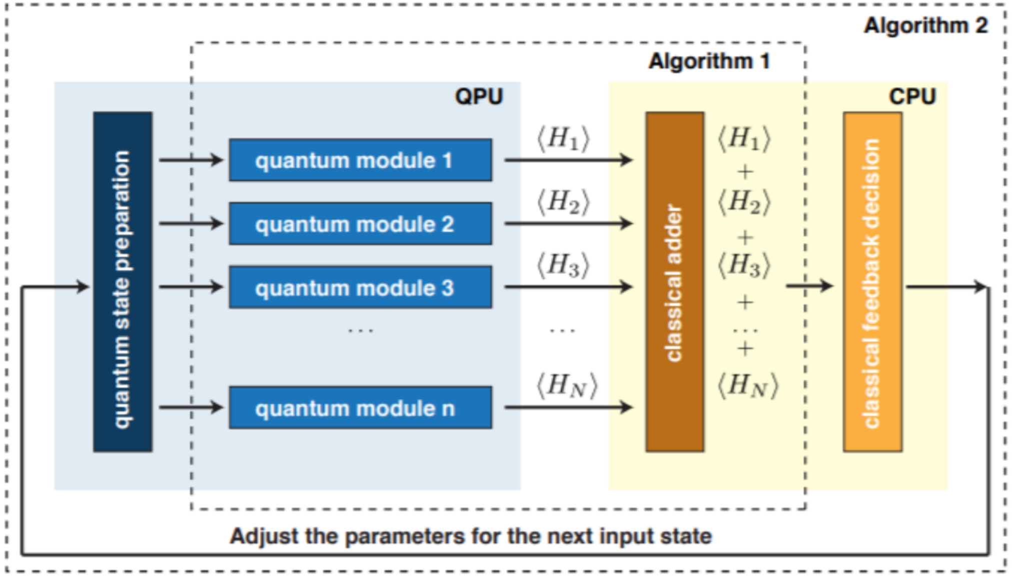

With serial processing, time scales linearly with number of Pauli words

BK transformation generates O(N^4) Pauli words

*Peruzzo *et al.* Nat. Comm. 5 (2014)

Unitary Coupled Cluster

Quantum computers cannot directly encode

$$U = \exp(T_1 + T_2 + \cdots)$$

$\Big\downarrow$ Trotterized

$$U \approx \left(\exp\left(\frac{T_1}{M}\right)\exp\left(\frac{T_2}{M}\right)\ldots\right)^M \quad M \geq 1$$

Even simplest fermionic operators are lengthy combination of Pauli terms

$$a_5^\dagger a_4^\dagger a_3 a_2 - a_2^\dagger a_3^\dagger a_4 a_5$$
$$\to \frac{i}{8}(x_2 y_4 + z_1 x_2 z_3 y_4 - y_2 x_4 - z_1 y_2 z_3 x_4 - y_2 x_4 z_5 - z_1 y_2 z_3 x_4 z_5 + x_2 y_4 z_5 + z_1 x_2 z_3 y_4 z_5)$$

Lengthy combinations of Pauli terms increases quantum circuit depth

LiH/STO-6G, C. Hempel *et al*. *Phys. Rev. X* **8**, 031022 (2018) taken from Dr. **Scott N. Genin**'s presentation

Qubit Coupled Cluster Method

$$\Psi(\tau,\omega) = \hat{U}(\tau)|\omega\rangle$$

General form of qubit methods

$$\hat{U}(\tau) = \prod_{k}^{N} \exp\left(\frac{i\tau_k \hat{P}_k}{2}\right)$$

$\hat{P}$ is Pauli word entanglers

$$E(\tau,\omega) \leq \langle\omega|U(\tau)^{\dagger}\hat{H}U(\tau)|\omega\rangle$$

Variational search
for ground state

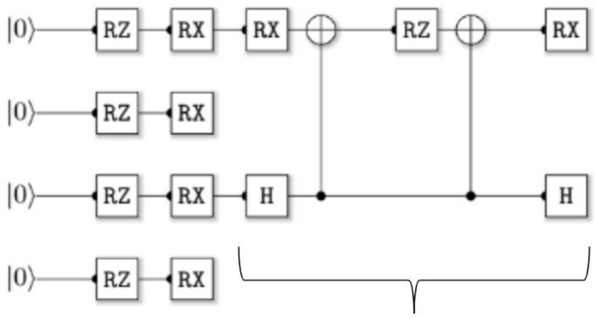

$$\hat{P} = y_0 x_2$$

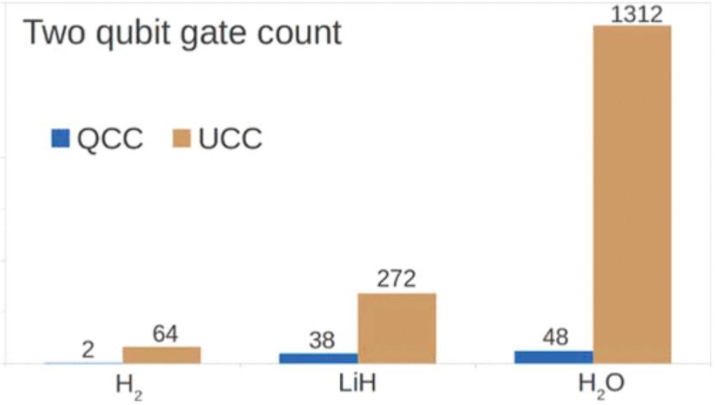

https://pubs.acs.org/doi/abs/10.1021/acs.jctc.8b00932

Feature	IBM (Gate-based circuit)	D-Wave (Annealer)
기본 아키텍처	Unitary gate fidelity 최우선	아날로그 최적화 과정
Coupler 필요성	초기에는 불필요 (오히려 노이즈 증가)	J_{ij} 자체가 문제 정의 → 필수
Depth/Error 요구	매우 엄격 (~10^{-3})	상대적으로 완화됨
Josephson 소자	사용	사용
Tunable coupler 도입	최근 (Heron generation)	10년 이상 전부터
이유	Flux 노이즈 억제 기술이 이제야 완성	본질적으로 coupler가 계산의 핵심

항목	양자 어닐러	Gate-based VQE
노이즈의 역할	local minima 탈출을 돕기도 함 (thermal activation + tunneling)	local minima 생성 (noise dips)
global minimum 접근	잘 됨	거의 불가능
algorithm 구조	energy landscape를 자연스럽게 따라감	optimizer가 landscape를 보고 gradient 추정
노이즈의 방향	에너지 landscape를 “부드럽게” 함	landscape를 “찢고 갈라짐”
scaling	매우 큼 (수 천~수 만 qubits 가능)	현재 수십 qubits 수준
실제 적용 사례	물리적 최적화, 큰 문제 성공 사례 많음	chemistry/물리 문제에서 실제 성공 거의 없음

Hydrogen Molecule

C. Quantum Annealing Example : Hydrogen model

- The electronic structure problem and its mapping on an Ising Hamiltonian

$$\rightarrow H = -\underbrace{\sum_{i} \frac{\nabla_i^2}{2}}_{\text{Kinetic Energy of electrons}} - \underbrace{\sum_{i,A} \frac{Z_A}{|r_i - R_A|}}_{\text{Coulomb interaction btw electrons \& nuclei}} + \underbrace{\sum_{i,j} \frac{1}{|r_i - r_j|}}_{\text{Coulomb interaction btw electrons}}$$

M : nuclei & N : electrons

r_i : position of electrons

M_A : mass in atomic units of the nuclei

R_A : position in atomic units of the nuclei

Z_A : charge in atomic units of the nuclei

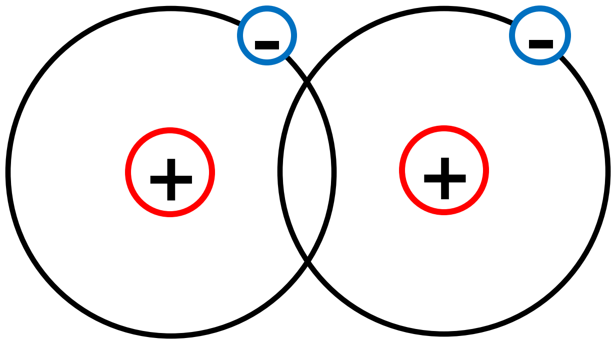

$\langle \mathbf{H_2} \rangle$

C. Quantum Annealing Example : Hydrogen model

- The electronic structure problem and its mapping on an Ising Hamiltonian

$$\rightarrow \ \mathrm{H} = \sum_{\mathrm{i,j}} \mathrm{h_{ij}} \underline{\mathrm{a_j}^{+}\mathrm{a_i}} + \frac{1}{2} \sum_{\mathrm{i,j,k,l}} \mathrm{h_{ijkl}} \underline{\mathrm{a_i}^{+}\mathrm{a_j}^{+}\mathrm{a_k}\mathrm{a_l}}$$

$\mathrm{a_i}^{+}$: fermionic creation operator

$\mathrm{a_j}$: fermionic annihilation operator

$$\{\mathrm{a_i}, \mathrm{a_j}^{+}\} = \delta_{ij}$$

$$\mathrm{h_{ij}} = \left\langle \psi_i \middle| -\frac{\nabla_i^{\,2}}{2} - \sum_A \frac{Z_A}{|r_i - R_A|} \middle| \psi_j \right\rangle \quad \& \quad \mathrm{h_{ij}}_{kl} = \left\langle \psi_i \psi_j \middle| \frac{1}{|r_i - r_j|} \middle| \psi_k \psi_l \right\rangle$$

** **fermionic creation & annihilation** ––→ **Pauli matrice**

arXiv:1811.05256

B. Hydrogen molecule model

Problem Parameters | Solution | Timing

QPU_SAMPLING_TIME
120.12 ms

QPU_ANNEAL_TIME_PER_SAMPLE
20.0 µs

QPU_READOUT_TIME_PER_SAMPLE
79.54 µs

QPU_ACCESS_TIME
135.87916 ms

QPU_ACCESS_OVERHEAD_TIME
1.18884 ms

QPU_PROGRAMMING_TIME
15.75916 ms

QPU_DELAY_TIME_PER_SAMPLE
20.58 µs

TOTAL_POST_PROCESSING_TIME
20.0 µs

POST_PROCESSING_OVERHEAD_TIME
20.0 µs

Timing Documentation

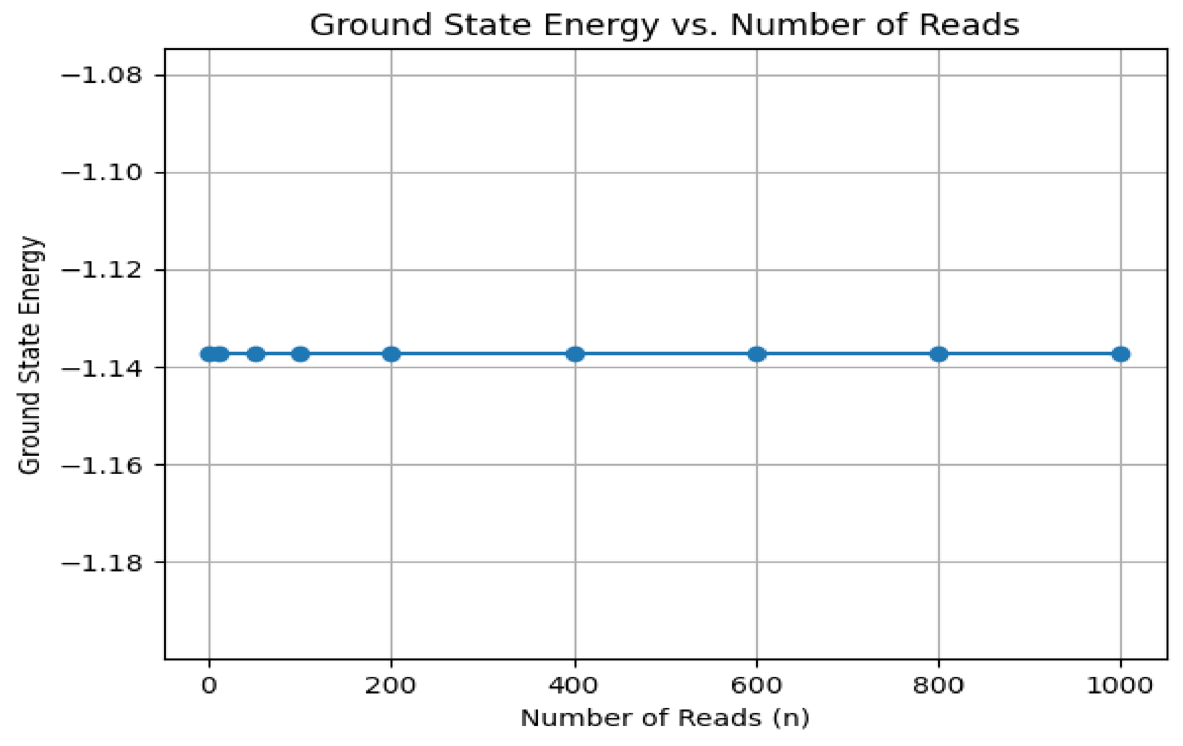

- Quantum Annealing using D wave

: −1.137308 hartree

1hartree = 27.2114eV

$1\text{hartree} = 27.2114\text{eV}$

- Classical Eigensolver : -1.137306 hartree 10.21s
- Variational Quantum Eigensolver : -1.137306 hartree 16.79s
- Quantum Annealing simulation : -1.137306 hartree 17.69s

Quantum Computing Applications

$\mathrm{D-Wave\ Quantum\ Computer}$

A. Introduction to D – Wave Quantum Computer

3) Annealing

$$H_{Ising} = \underbrace{-\frac{A(s)}{2}\left(\sum_i \hat{\sigma}_x^{(i)}\right)}_{\text{Initial state}} + \underbrace{\frac{B(s)}{2}\left(\sum_i h_i \hat{\sigma}_z^{(i)} + \sum_{i,j} J_{i,j}\hat{\sigma}_z^{(i)}\hat{\sigma}_z^{(j)}\right)}_{\text{Final state}}$$

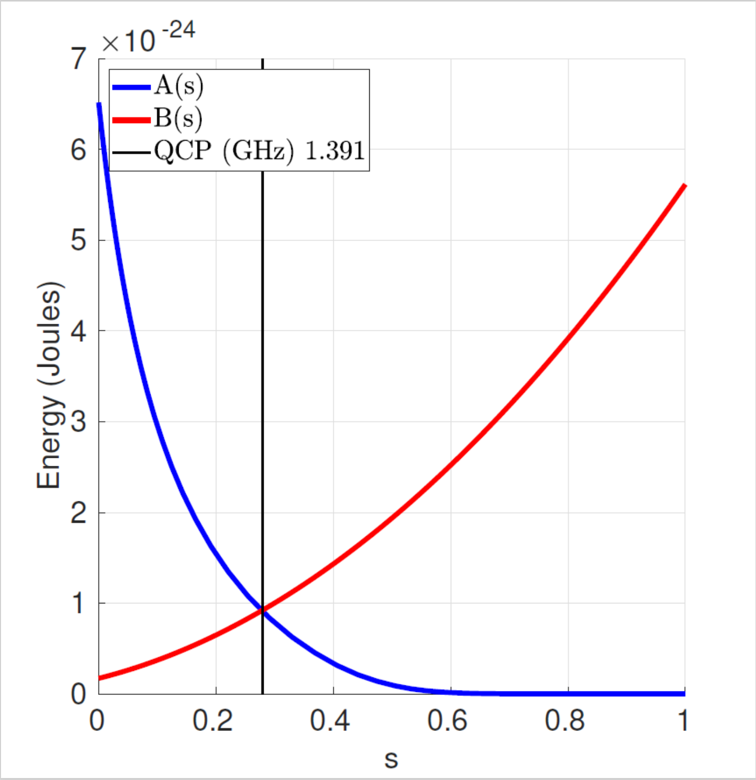

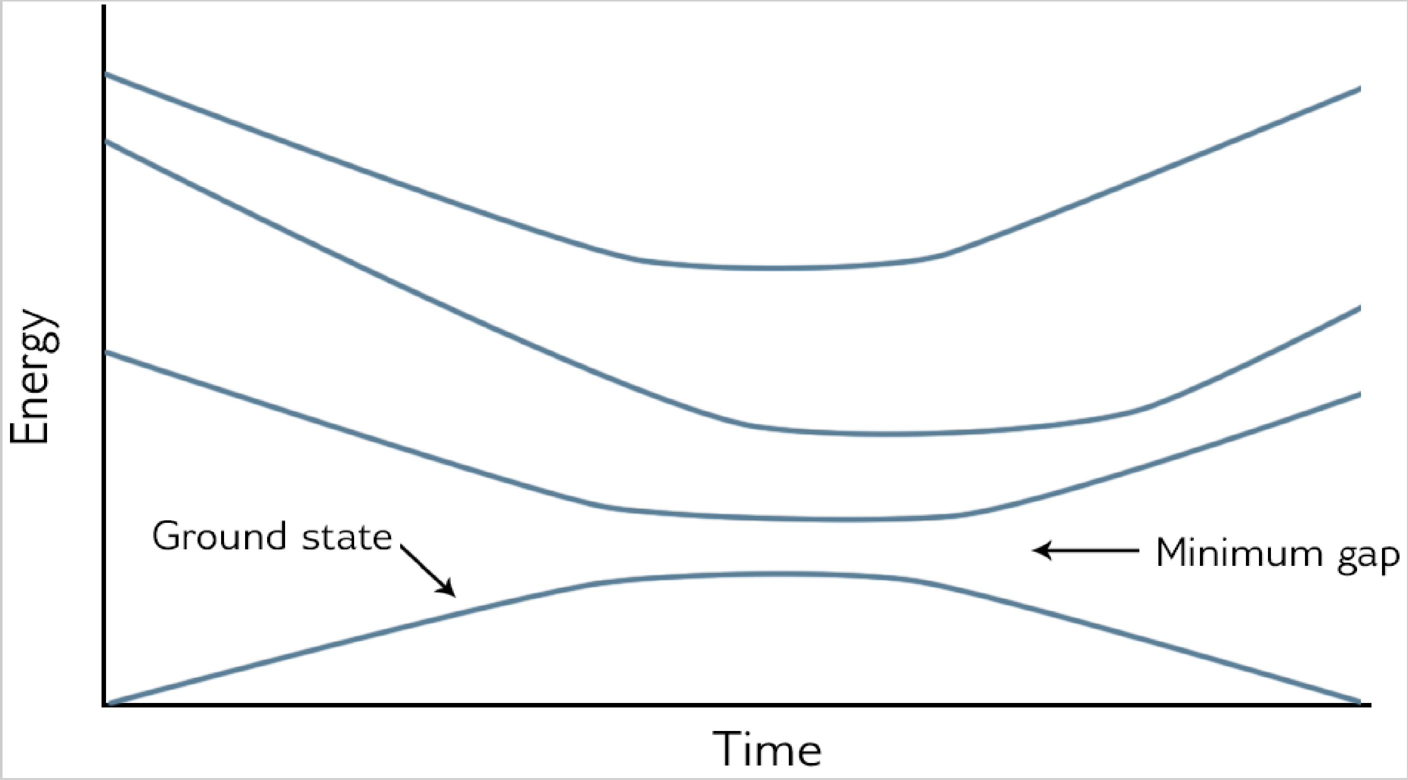

Google 양자우월성 증명

방정호 박사님(한국전자통신연구원) 발표자료

Google's quantum supremacy proof

The leading quantum supremacy proposals:

- Boson Sampling
- Fourier Sampling
- Instantaneous Quantum Polynomial-time (IQP)
- Random Circuit Sampling (RCS)

	Worst-case hardness	Average-case hardness	Anti-Concentration	Experimentally Feasible
Boson Sampling	OK	OK		
Fourier Sampling	OK	OK		
IQP	OK		OK	
RCS	OK	OK	OK	OK

[Nature Physics **15**, 159 (2019)] [Nature Physics **14**, 595 (2018)]

Theoretical proof

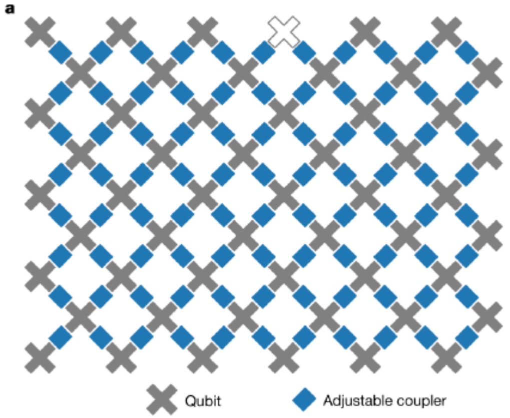

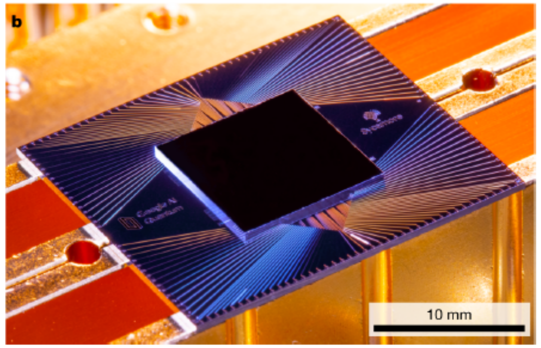

Google's Sycamore Processor

[Nature **574**, 505 (2019)]

Hardware demonstration

Interplay between software and NISQ hardware

Article

Quantum supremacy using a programmable superconducting processor

https://doi.org/10.1038/s41586-019-1666-5

Received: 22 July 2019

Accepted: 20 September 2019

Published online: 23 October 2019

Frank Arute[1], Kunal Arya[1], Ryan Babbush[1], Dave Bacon[1], Joseph C. Bardin[1,2], Rami Barends[1], Rupak Biswas[3], Sergio Boixo[1], Fernando G. S. L. Brandao[1,4], David A. Buell[1], Brian Burkett[1], Yu Chen[1], Zijun Chen[1], Ben Chiaro[5], Roberto Collins[1], William Courtney[1], Andrew Dunsworth[1], Edward Farhi[1], Brooks Foxen[1,5], Austin Fowler[1], Craig Gidney[1], Marissa Giustina[1], Rob Graff[1], Keith Guerin[1], Steve Habegger[1], Matthew P. Harrigan[1], Michael J. Hartmann[1,6], Alan Ho[1], Markus Hoffmann[1], Trent Huang[1], Travis S. Humble[7], Sergei V. Isakov[1], Evan Jeffrey[1], Zhang Jiang[1], Dvir Kafri[1], Kostyantyn Kechedzhi[1], Julian Kelly[1], Paul V. Klimov[1], Sergey Knysh[1], Alexander Korotkov[1,8], Fedor Kostritsa[1], David Landhuis[1], Mike Lindmark[1], Erik Lucero[1], Dmitry Lyakh[9], Salvatore Mandrà[3,10], Jarrod R. McClean[1], Matthew McEwen[5], Anthony Megrant[1], Xiao Mi[1], Kristel Michielsen[11,12], Masoud Mohseni[1], Josh Mutus[1], Ofer Naaman[1], Matthew Neeley[1], Charles Neill[1], Murphy Yuezhen Niu[1], Eric Ostby[1], Andre Petukhov[1], John C. Platt[1], Chris Quintana[1], Eleanor G. Rieffel[3], Pedram Roushan[1], Nicholas C. Rubin[1], Daniel Sank[1], Kevin J. Satzinger[1], Vadim Smelyanskiy[1], Kevin J. Sung[1,13], Matthew D. Trevithick[1], Amit Vainsencher[1], Benjamin Villalonga[1,14], Theodore White[1], Z. Jamie Yao[1], Ping Yeh[1], Adam Zalcman[1], Hartmut Neven[1] & John M. Martinis[1,5*]

The promise of quantum computers is that certain computational tasks might be executed exponentially faster on a quantum processor than on a classical processor[1]. A fundamental challenge is to build a high-fidelity processor capable of running quantum algorithms in an exponentially large computational space. Here we report the use of a processor with programmable superconducting qubits[2–7] to create quantum states on 53 qubits, corresponding to a computational state-space of dimension 2^{53} (about 10^{16}). Measurements from repeated experiments sample the resulting probability distribution, which we verify using classical simulations. Our Sycamore processor takes about 200 seconds to sample one instance of a quantum circuit a million times—our benchmarks currently indicate that the equivalent task for a state-of-the-art classical supercomputer would take approximately 10,000 years. This dramatic increase in speed compared to all known classical algorithms is an experimental realization of quantum supremacy[8–14] for this specific computational task, heralding a much-anticipated computing paradigm.

In the early 1980s, Richard Feynman proposed that a quantum computer would be an effective tool with which to solve problems in physics and chemistry, given that it is exponentially costly to simulate large quantum systems with classical computers[1]. Realizing Feynman's vision poses substantial experimental and theoretical challenges. First, can a quantum system be engineered to perform a computation in a large enough computational (Hilbert) space and with a low enough error rate to provide a quantum speedup? Second, can we formulate a problem that is hard for a classical computer but easy for a quantum computer? By computing such a benchmark task on our superconducting qubit processor, we tackle both questions. Our experiment achieves quantum supremacy, a milestone on the path to full-scale quantum computing[8–14].

In reaching this milestone, we show that quantum speedup is achievable in a real-world system and is not precluded by any hidden physical laws. Quantum supremacy also heralds the era of noisy intermediate-scale quantum (NISQ) technologies[15]. The benchmark task we demonstrate has an immediate application in generating certifiable random numbers (S. Aaronson, manuscript in preparation); other initial uses for this new computational capability may include optimization[16,17], machine learning[18–21], materials science and chemistry[22–24]. However, realizing the full promise of quantum computing (using Shor's algorithm for factoring, for example) still requires technical leaps to engineer fault-tolerant logical qubits[25–29].

To achieve quantum supremacy, we made a number of technical advances which also pave the way towards error correction. We

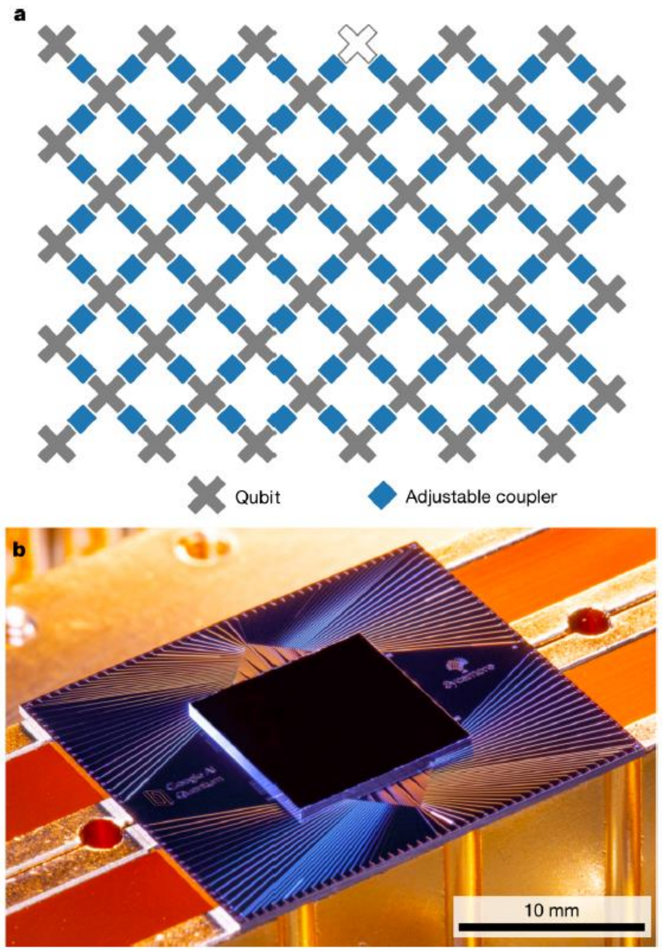

Google's Sycamore Processor

Google 양자우월성 증명

방정호 박사님(한국전자통신연구원) 발표자료

nature physics
ARTICLES
https://doi.org/10.1038/s41567-018-0124-x

Characterizing quantum supremacy in near-term devices

Sergio Boixo[1*], Sergei V. Isakov[2], Vadim N. Smelyanskiy[1], Ryan Babbush[1], Nan Ding[1], Zhang Jiang[3,4], Michael J. Bremner[5], John M. Martinis[6,7] and Hartmut Ne

A critical question for quantum computing in the near future is whether q
a well-defined computational task beyond the capabilities of supercompu
quantum supremacy requires a reliable evaluation of the resources requir
propose the task of sampling from the output distribution of random quan
acy. We extend previous results in computational complexity to argue th
a classical computer. We introduce cross-entropy benchmarking to obt
dynamics. This can be estimated and extrapolated to give a success metri
the computational cost of relevant classical algorithms and conclude that
a two-dimensional lattice of 7×7 qubits and around 40 clock cycles. This
gates (0.05% for one-qubit gates), and it would demonstrate the basic bu

nature physics
ARTICLES
https://doi.org/10.1038/s41567-018-0318-2

On the complexity and verification of quantum random circuit sampling

Adam Bouland[1], Bill Fefferman[1,2*], Chinmay Nirkhe[1] and Umesh Vazirani[1]

A critical milestone on the path to useful quantum computers is the demonstration of a quantum computation that is prohibitively hard for classical computers—a task referred to as quantum supremacy. A leading near-term candidate is sampling from the probability distributions of randomly chosen quantum circuits, which we call random circuit sampling (RCS). RCS was defined with experimental realizations in mind, leaving its computational hardness unproven. Here we give strong complexity-theoretic evidence of classical hardness of RCS, placing it on par with the best theoretical proposals for supremacy. Specifically, we show that RCS satisfies an average-case hardness condition, which is critical to establishing computational hardness in the presence of experimental noise. In addition, it follows from known results that RCS also satisfies an anti-concentration property, namely that errors in estimating output probabilities are small with respect to the probabilities themselves. This makes RCS the first proposal for quantum supremacy with both of these properties. Finally, we also give a natural condition under which an existing statistical measure, cross-entropy, verifies RCS, as well as describe a new verification measure that in some formal sense maximizes the information gained from experimental samples.

Quantum Computing Applications

$\mathrm{D-Wave\ Quantum\ Computer}$

A. Introduction to D – Wave Quantum Computer

3) Annealing

$$H_{\text{Ising}} = \underbrace{-\frac{A(s)}{2}\left(\sum_i \hat{\sigma}_x^{(i)}\right)}_{\text{Initial state}} + \underbrace{\frac{B(s)}{2}\left(\sum_i h_i \hat{\sigma}_z^{(i)} + \sum_{i,j} J_{i,j}\hat{\sigma}_z^{(i)}\hat{\sigma}_z^{(j)}\right)}_{\text{Final state}}$$

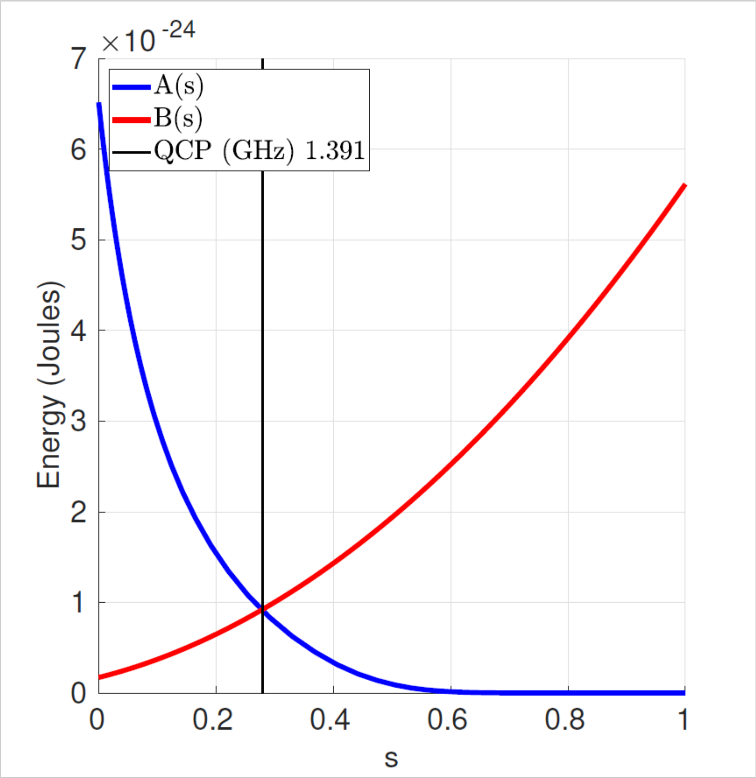

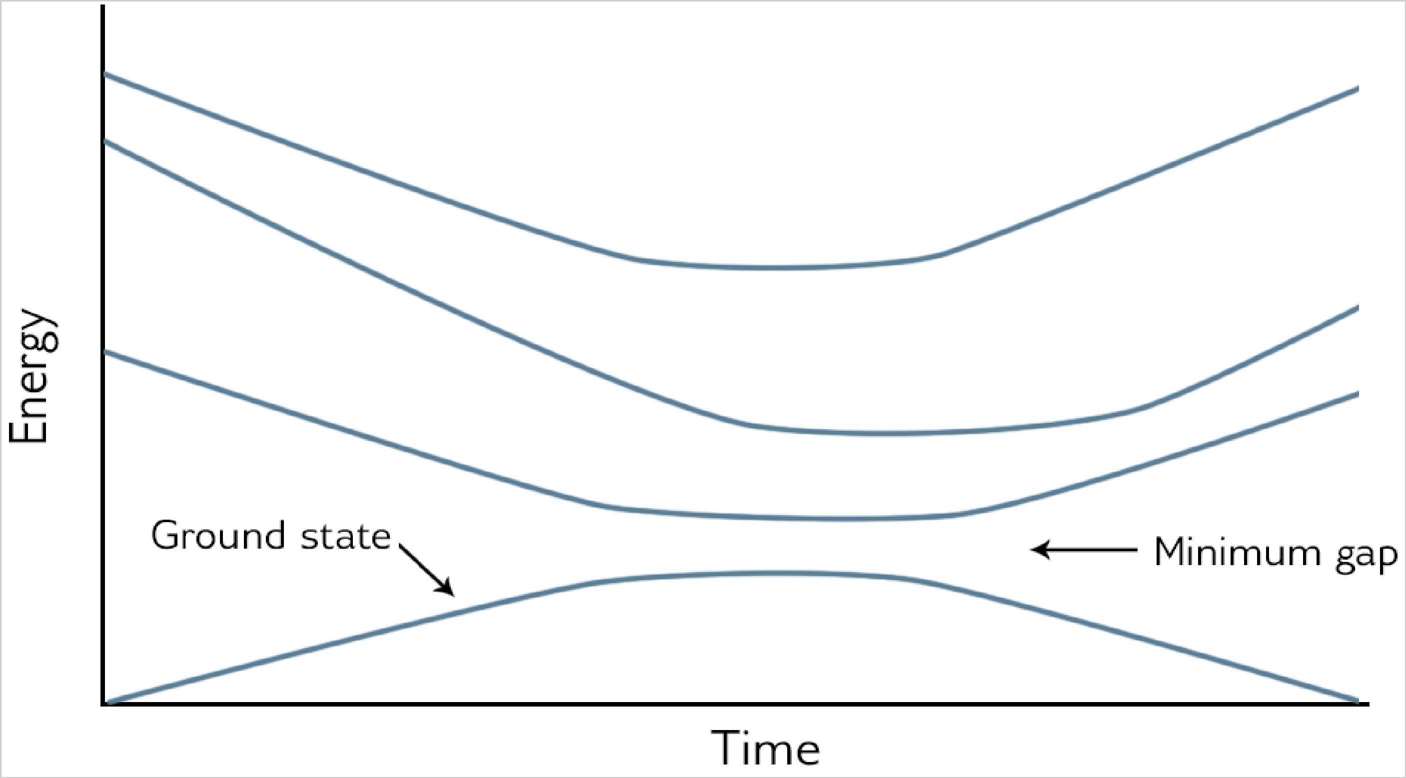

ibm_fez

Details

Qubits	2Q error (best)	2Q error (layered)	CLOPS
156	1.49E-3	4.52E-3	220K
Status	**Region**	**QPU version**	**Processor type**
Online	Washington DC (us-east)	1.3.27	Heron r2
Basis gates	**Pending jobs**	**Median CZ error**	**Median SX error**
cz, id, rx, rz, rzz, sx, x	0	2.643E-3	2.593E-4
Median readout error	**Median T1**	**Median T2**	
9.644E-3	142.41 us	98.43 us	

3. Helium–4 (^{4}He) — 2-body cluster EFT / Minnesota potential 기반

^{4}He(VQE)의 대표 연구:

- JORDAN–LEE–PRESKILL approach
- Roggero, PRC 105, 024318 (2022)
- Stetcu et al., PRL 126, 062501 (2021)

이들은 **4체(4-body) Schrödinger 문제 → 2-body effective Hamiltonian**을 사용.

◆ 대표적인 ^{4}He 유효 Hamiltonian 형태

가장 널리 인용되는 4×4 행렬 예:

$$H_{^4He} = \begin{pmatrix} 5.907 & -1.123 & 0 & 0 \\ -1.123 & 3.214 & -0.954 & 0 \\ 0 & -0.954 & 2.438 & -0.852 \\ 0 & 0 & -0.852 & 1.894 \end{pmatrix} \text{MeV}$$

이 Hamiltonian은

- “Minnesota nucleon–nucleon potential”
- “model space truncation (harmonic oscillator basis)”

을 적용했을 때 대표적으로 나오는 구조입니다.

VQE에서는 보통 이 행렬을 **파울리 행렬 합**으로 변환해 2–3 qubit에 매핑합니다.

✅ 4. Helium–3 (^3He)

^3He의 경우 양자컴 연구는 많지 않지만,
NCSM (No-Core Shell Model) → 2–3 qubit subspace projection 형태가 등장합니다.
대표적인 형태는:

$$H_{^3He} = \begin{pmatrix} -8.05 & 1.12 & 0.00 \\ 1.12 & -6.26 & 0.92 \\ 0.00 & 0.92 & -5.11 \end{pmatrix} \text{ MeV}$$

(하모닉 진동자 기반의 truncation)